DNA damage signaling networks: from stem cells to cancer

Carreras Puigvert, J.

Chapter 5

Mapping DNA damage response signaling networks in ES cells - downregulation of CSNK1a1 leads to enhanced Wnt signaling that acts as a brake on p53-mediated apoptosis.

Manuscript in preparation

Mapping DNA damage response networks in ES cells – enhanced Wnt-signaling through downregulation of CSNK1a1 attenuates p53-mediated apoptosis

Jordi C Puigvert*[1], Louise von Stechow*[1], Ramakrishnaiah Siddappa*[1], Alex Pines[2], Jesper V Olson[3], Harry Vrieling[2], Leon HF Mullenders[2], Bob van de Water[1], and Erik HJ Danen[1]**

[1] Division of Toxicology, Leiden/Amsterdam Center for Drug Research, Leiden University, The Netherlands
[2] Department of Toxicogenetics, Leiden University Medical Center, The Netherlands
[3] Department of Proteomics, Novo Nordisk Foundation Center for Protein Research, Faculty of Health Sciences, University of Copenhagen, Denmark.

*Equal contribution **Corresponding author

SUMMARY

Damaged DNA contributes to aging when (stem) cells accumulate cytotoxic lesions and to cancer through mutagenic lesions. It is also the mechanism of action of anticancer radio- and chemotherapy. The anticancer drug, cisplatin causes DNA cross-links, stalled replication forks, and as a consequence double strand breaks. We analyze the signaling response to such broad-range DNA damage in pluripotent stem cells where repair pathways and triggering cell death when damage is beyond repair must be particularly robust. In an RNAi screen targeting kinases, phosphatases, and transcription factors we identify cisplatin response modifiers in embryonic stem (ES) cells. A number of such modifiers are found to play similar roles in p53 mutant breast cancer cells. Subsequently, the RNAi screen is combined with global transcriptomics and phospho-proteomics (SILAC) to build integrated networks. In addition to the expected pathways, these point to alterations in self-renewal signaling. In particular, our findings demonstrate that genotoxic stress in ES cells elicits Wnt signaling through downregulation of the negative regulator CSNK1a1 to constrain p53-mediated apoptosis.

INTRODUCTION

It is estimated that cells suffer approximately 100,000 DNA insults per day. Ionizing radiation (IR), X-rays, UV-light, oxygen radicals, and various chemicals modify DNA bases or cause breaks. Since damaged DNA, in contrast to RNA or proteins cannot be recycled, a highly complex DNA repair machinery has evolved. Nucleotide mismatches, deletions, inter- or intra-strand cross-links, and single (SSB)- or double strand breaks (DSB) each trigger a specific version of the "DNA damage response" (DDR) (Jackson & Bartek, 2009; Ciccia & Elledge, 2010). The DDR is an intricate network of signaling pathways conserved in eukaryotes. Its prime functions are damage repair; slowing down the cell cycle to allow time for repair; and, if damage is too severe, initiation of senescence or apoptosis. The fact that the DDR is not perfect may contribute to genetic variation in the population but also contributes to aging when (stem) cells accumulate cytotoxic lesions, and sets the stage for cancer when cells acquire mutagenic lesions (Hoeijmakers, 2009).

The majority of lesions induced by the widely used genotoxic anticancer drug, cisplatin (CP), are inter-strand cross-links (ICL) (Jordan & Carmo-Fonseca, 2000). ICL can be repaired through the Fanconi anemia pathway, which involves ubiquitination and recruitment of Fanconi proteins to promote processing of the ICL lesion (Räschle *et al*, 2008). ICL also cause stalled replication forks and generation of DSB as secondary lesions. Single strand DNA at stalled replication forks and exposed during DSB processing triggers activation of the kinase ATR through a signaling cascade involving ATRIP, Rad17, the 9-1-1 complex (Rad9, Ra1, Hus1), and TOPBP1(Cortez *et al*, 2001; Zou & Elledge, 2003; Parrilla-Castellar *et al*, 2004). DSBs can be repaired through homologous recombination or non-homologous end-joining and trigger activation of the kinase ATM through the Mre11/Rad50/Nbs1 complex and of the kinase DNA-PK through the Ku70/Ku80 complex (Hakem, 2008; Lombard *et al*, 2005). The DSB repair proteins are recruited into DSB repair foci, which are typically marked by 53BP1 and phosphorylated histone variant H2AX (γH2AX) (Bartek *et al*, 2007). Finally, CP induces ER stress and oxidative stress, which may indirectly cause DNA base modifications triggering alternative DDR pathways (Jordan & Carmo-Fonseca, 2000). Thus, repair of CP-induced lesions is a highly pleiotropic process that includes components of the DSB repair pathways.

It is important that i) repair mechanisms are coordinated with other cellular processes such as transcription and cell cycle progression and ii) that cells in which excessive DNA damage cannot be repaired are removed to prevent tissue damage and prevent accumulation of mutagenic lesions that would otherwise lead to cancer. For these reasons, besides repair pathways whose components concentrate at the site of damage, the DDR includes a more global signaling network. For instance, ATR and ATM phosphorylate substrates in DSB repair foci (e.g. Mdc1, Nbs1, BRCA, H2AX and many others) but also the checkpoint kinases Chk1 and Chk2 that diffuse throughout the nucleus and initiate a second wave of signaling involved in cell cycle arrest and apoptosis. ATM, ATR, Chk1, and Chk2

have all been implicated in activation of p53, a critical transcription factor in the DDR that monitors the extent and duration of damage and activates a cellular program leading to cell cycle arrest, apoptosis, or senescence depending on its transcriptional targets (Kodama *et al*, 2010).

Over the past 10 years, the orchestrated network of DDR signaling cascades has expanded considerably and the current view on it most likely is still incomplete (Polo & Jackson, 2011; Blanpain *et al*, 2011; Harper & Elledge, 2007; Matsuoka *et al*, 2007). RNAi screens in cancer cells have identified new regulators of genome stability, IR-induced DSB repair foci, and genotoxic stress-induced apoptosis (Arora *et al*, 2010; Kolas *et al*, 2007; MacKeigan *et al*, 2005; Paulsen *et al*, 2009). In stem cells, recent evidence shows that genotoxic stress elicits responses beyond those discussed above, including cell differentiation (Sherman *et al*, 2011). For instance, p53 activation in mouse embryonic stem (ES) can lead to repression of *Nanog*, a gene required for self-renewal (Lin *et al*, 2005). Such a differentiation response may act as safe guard to prevent passage of damaged DNA through the lineage. In the current study, we have combined global transcriptomics and phospho-proteomics (SILAC) with gene family wide RNAi screens targeting all known kinases, phosphatases, and transcription factors to unravel the DDR in ES cells treated with CP. In such pluripotent stem cells, which undergo self-renewal as well as differentiation and give rise to all cells in the body, repair pathways as well as pathways that trigger cell death when damage is beyond repair must be particularly robust. Our functional genomics identifies novel CP response modifying genes, several of which are found in subsequent validation screens to control survival and chemo-response of cancer cells. Integration of the different datasets points to known and new aspects of DDR, including marked changes in differentiation-associated signaling networks. However, we observe no signs of differentiation. Instead, an alternative mode of DNA-damage-induced Wnt signaling is identified that acts to suppress p53-mediated apoptosis in ES cells.

RESULTS

RNAi screen

In order to identify key mediators of the response to genotoxic stress in pluripotent stem cells, an RNAi screen targeting all known kinases, phosphatases, and transcription factors was performed in mouse ES cells. FACS for DNA content or ATP-based viability measurement showed 60-70% ES cell death after 24h 10μM CP treatment, which was prevented by the pan-Caspase inhibitor Z-VAD-fmk, pointing to CP-induced apoptosis (suppl Fig 1A,B). For the screen protocol, siRNA targeting Kif11 was used as transfection control, si-GFP and si-LaminA/C as negative controls, and we tested the effect of si-p53. The role of p53 in DDR in ES cells is debated (Aladjem *et al*, 1998; Sabapathy *et al*, 1997; Solozobova *et al*, 2009). si-Kif11 killed cells in the absence or presence of CP as expected and si-p53 copied the protective effect of Z-VAD-fmk in CP-treated cells while non of the negative controls had any effect (suppl Fig 1C). In conclusion, CP triggers a p53-mediated apoptotic response in mouse ES cells.

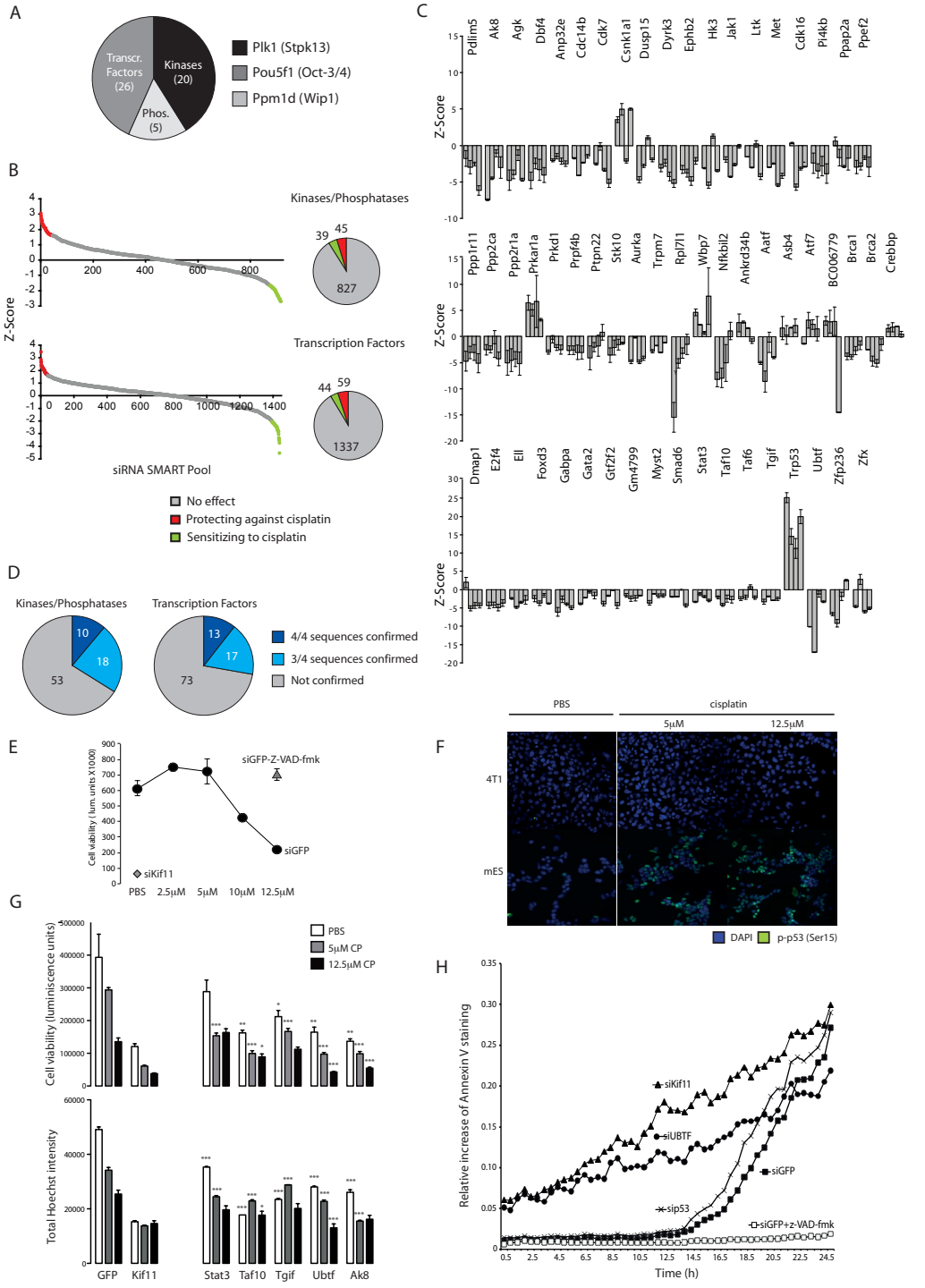

In the primary screen, 2,351 genes were silenced using SMARTpools and viability under control and 10μM CP conditions was determined. The average Z'factor (Boutros *et al*, 2006) of all CP-treated plates based on si-LaminA/C and si-p53 was ~0.5, indicating a strong signal to noise ratio (suppl Fig 1D). For

hit selection, we first excluded siRNAs that significantly reduced viability in control conditions. This list contained expected survival genes from all three gene families, such as Plk1, Oct-3/4, and Wip1 (Fig 1A; suppl Fig 1E). Ingenuity Pathway Analysis (IPA) was used to find predicted interacting molecules and a network was created from the enriched data set. Within this network canonical pathways involved in general survival and metabolism - including "insulin receptor signaling", "AMPK signaling", "mTor signaling", and "purine-metabolism" were overrepresented (suppl Fig 1F).

After exclusion of siRNAs affecting general survival, siRNAs were ranked against si-LaminA/C using Z-scores (Birmingham *et al*, 2009) and hits were defined as [absolute Z-Score>1.5; p<0.05]. Using these criteria, 104 SMARTpools protected against CP and 83 sensitized (suppl Table 1; Fig 1B). These hits entered a secondary deconvolution screen where hit confirmation was defined as at least 3 out of 4 individual siRNAs copying the effect of the SMARTpool with [absolute Z-Score>1.5; p<0.05]. In this way, 3% of all kinases, phosphatases, and transcription factors (~30% of the primary screen hits) were confirmed as CP response modifiers (Fig 1C,D; suppl Table 1). In an interaction-enriched network from these 58 high-confidence hits, canonical pathways were overrepresented that are associated with cancer, cell cycle and survival, and differentiation (Fig 2A-D).

Validation of hits in cancer cells

Tolerance to damaged DNA is a hallmark of cancer cells. Since the RNAi screen in ES cells pointed to cancer-associated canonical pathways, we explored the possibility that the identified siRNAs that sensitize ES cells to CP also impacted on survival or chemosensitivity of cancer cells. For this, all sensitizing siRNAs were screened in 4T1 breast cancer cells lacking a functional p53 response that could be killed by CP in a concentration-dependent fashion that was blocked by Z-VAD-fmk (Fig 1E,F). Intriguingly, several of the hits identified in ES cells also significantly suppressed viability / sensitivity of 4T1 cells (Fig 1G). Silencing of Stat3, which has been shown to be constitutively activated in over 50% of cancers, and for which inhibitors are in clinical trials (Jing & Tweardy, 2005; Yang *et al*, 2010), resulted as expected, in sensitization of 4T1 cells to CP. Knock down of the RNA polymerase I-specific transcription factor UBTF (Upstream Binding Transcription Factor), which

Figure 1. RNAi screen for CP response modifiers in ES cells and verification of selected hits in 4T1 cells. (A) Distribution of SMARTpools from indicated gene families affecting general cell viability under control (PBS) condition with known survival genes for each family. **(B)** Graphs show Z-score ranking in primary screen of SMARTpools after exclusion of those affecting general viability. Pie diagrams show number of SMARTpools protecting against CP (red) or sensitizing to CP (green) according to [absolute Z-Score>1.5; p<0.05]. **(C)** Verification of hits from primary screen by deconvolution using 4 individual siRNAs against each target gene. **(D)** Number of primary hits confirmed (dark & light blue) and rejected (grey). **(E)** Titration of CP-induced apoptosis in 4T1 cells showing rescue by z-VAD-fmk and killing by si-Kif11 as transfection control. **(F)** Induction of p53 pSer15 in ES cells but not in 4T1 cells in response to CP treatment. **(G)** Effect of indicated siRNAs on viability of 4T1 cells in absence or presence of indicated concentrations of CP analyzed by ATPlite assay (top) or Hoechst intensity (bottom). **(H)** Real time imaging of Annexin V-FITC binding to 4T1 cells during treatment with 5 μM CP in presence or absence of indicated siRNAs.

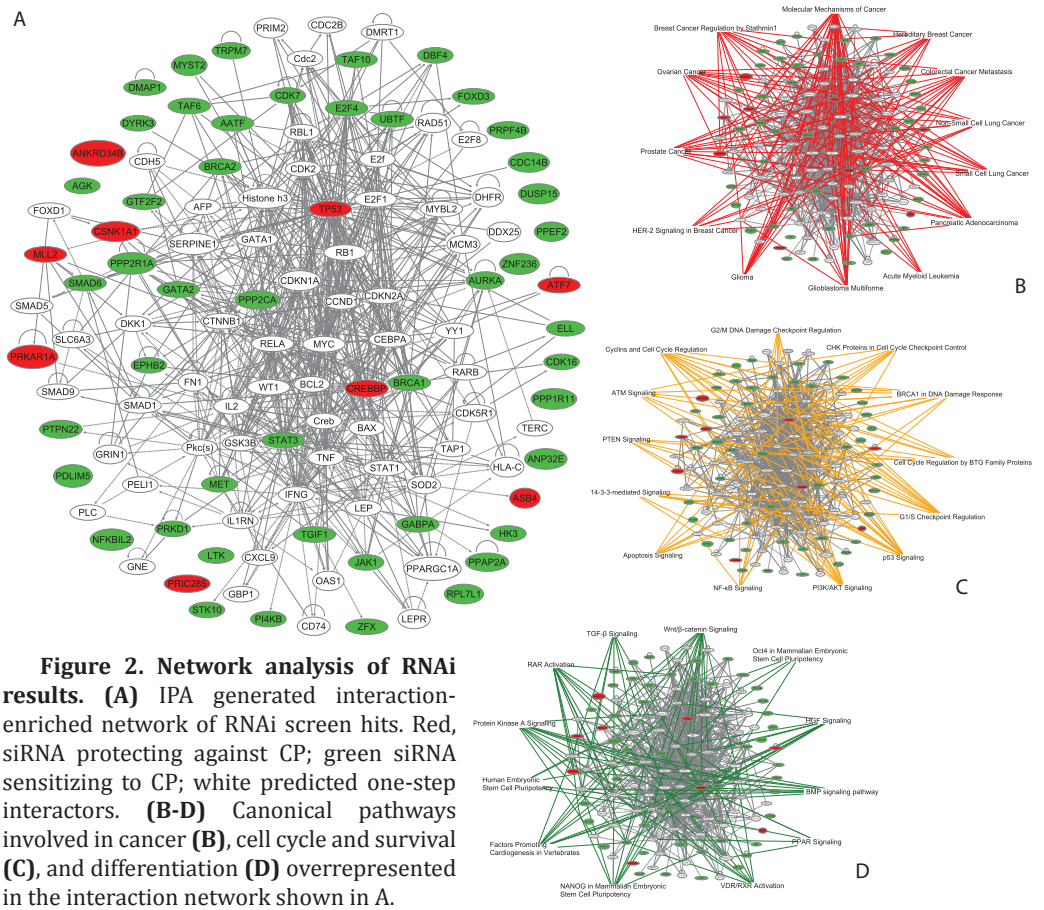

Figure 2. Network analysis of RNAi results. (A) IPA generated interaction-enriched network of RNAi screen hits. Red, siRNA protecting against CP; green siRNA sensitizing to CP; white predicted one-step interactors. **(B-D)** Canonical pathways involved in cancer **(B)**, cell cycle and survival **(C)**, and differentiation **(D)** overrepresented in the interaction network shown in A.

is up-regulated in hepatocellular carcinomas (Huang *et al*, 2002), also enhanced background and CP-induced translocation of phosphatidyl-serine to the outer membrane leaflet, confirming the anti-apoptotic effect of this molecule (Fig 1H). TAF 10 together with Transcription factor IID (TFIID) are known to regulate basal transcription. Like UBTF, TAF10 silencing significantly induced loss of viability in 4T1 cells in PBS as well as in CP conditions.

Silencing transforming growth-interacting factor (TGIF), a homeobox transcriptional repressor involved in proliferation and differentiation (Hamid & Brandt, 2009; Liu, 2008) also suppressed 4T1 viability in both PBS and CP conditions (Figure 1G). Approximately 35% of TGIF target genes regulate cellular proliferation, differentiation and apoptosis, 18% have been involved in hematopoiesis, and 15% in various types of cancer (Hamid & Brandt, 2009). TGIF negatively regulates TGFβ signaling and interacts with Smads.

Activation of cAMP-mediated protein kinase signaling is known to rescue genotoxic stress-induced apoptosis (Naderi *et al*, 2009; Orlov *et al*, 1999). In line with this observation, knocking down adenylate kinase 8 (Ak8) which phosphorylates AMP (Panayiotou *et al*, 2011) induced sensitization to CP. Taken together, the RNAi screen, in addition

to ES cell specific hits has identified CP response modifiers that play similar roles in cancer cells lacking a functional p53 response. Further investigation of the identified molecules in multiple cancer cell types will show if these represent valuable anticancer targets.

Integration of functional genomics with transcriptomics and phosphoproteomics – role for DSB repair

In parallel to the transcription factor and kinase/phosphatase RNAi screens, we used micro-array and SILAC to map global changes in mRNA expression and protein phosphorylation in response to CP treatment. ES cells were exposed to vehicle or 1, 5, or 10μM CP for 8 h, followed by RNA isolation. Cells analyzed from parallel plates of the same experiment confirmed concentration-dependent induction of apoptosis at 24h (Fig 3A-B). A concentration-dependent induction of differentially expressed genes (DEGs; p<0.05) was observed and 2269 DEGs were identified at 10μM exposure. 29 of the 47 DEGs already responding to 1μM CP, showed a concentration-dependent increase in fold-change including known p53-targets such as Mdm2 and Btg2, in agreement with a p53-mediated response to CP in ES cells (suppl Fig 1C, Fig 3C,D).

The SILAC experiment is described in detail elsewhere (Pines *et al*, 2011). In short, isotope-labeled

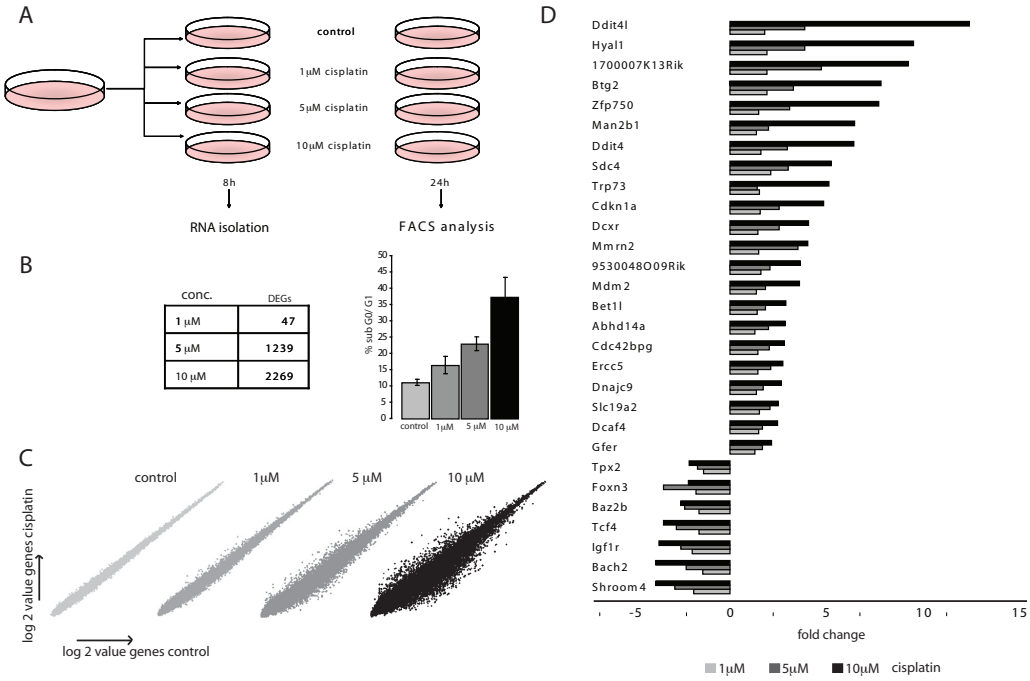

Figure 3. Transcriptomics analysis of ES cells treated with CP. (A) Schematic representation of the experiments. **(B)** Increase in differentially expressed genes (DEGs; p-value<0.05) after 8h treatment with indicated concentrations CP and verification of increased apoptosis in parallel samples at 24h treatment. **(C)** Concentration-dependent increase in DEGs. **(D)** DEGs identified in all 3 CP concentrations showing dose-response.

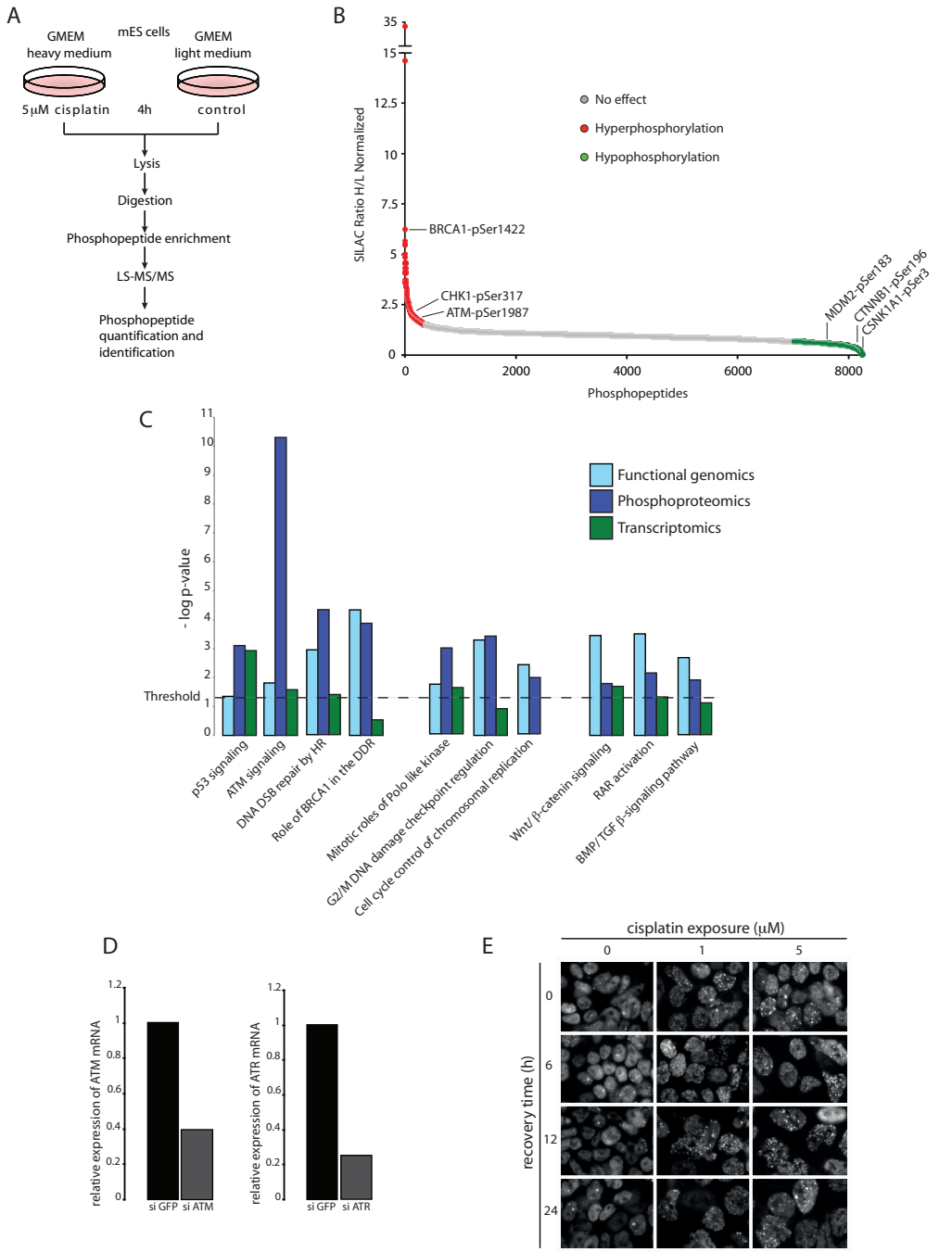

Figure 4. Phosphoproteomics (SILAC) analysis of ES cells treated with CP and canonical pathways shared between datasets. (A) Schematic representation of the experiments. **(B)** Ranking of phospho-peptides. Examples of peptides that were differentially phosphorylated [ratio<0.67 or ratio>1.5 and p<0.05] are indicated. **(C)** Canonical pathways significantly enriched in functional genomics (light blue), transcriptomics (green) and phosphoproteomics (dark blue). **(D)** qPCR validation of knockdown of ATM (left) and ATR (right). **(E)** Induction of DNA damage repair foci marked by 53BP1 staining in response to treatment with 1-5 μM CP and lack of disappearance of foci during indicated recovery periods in absence of CP.

amino acids were used to differentiate between proteins isolated from untreated ES cells and ES cells treated with 5μM CP for 4h. Isolated peptide mixtures were enriched for phosphopeptides on a titanium column and samples were analyzed by tandem mass spectometry (Fig 4A). Of the 8,251 identified phosphopeptides, 1,612 showed differential phosphorylation with criteria [ratio<0.67 or ratio>1.5; p<0.05] (Fig 4B).

Interaction-enriched networks were generated from the DEGs and from the 1025 proteins yielding differentially phosphorylated peptides. In agreement with the functional genomics analysis (Fig 2), canonical pathways involved in cancer, cell cycle & survival, and differentiation were enriched (suppl Table 2). Out of the most significantly enriched canonical pathways (p<0.05; Fisher's exact test) several were involved in DSB repair, e.g. "DSB repair by HR", "BRCA1 in DDR", and "ATM signaling" (Fig 4C). CP-induced DNA-damage is highly complex comprising inter- and intrastrand crosslinks, stalled replication forks, and subsequent DSB. DSB repair signaling was initiated as seen by an ATM-associated protein phosphorylation signature (including autophosphorylation of ATM on Ser1987; Fig 4B,C; suppl Table 3) and formation of repair foci (53BP1, Rad51, γH2AX) (Fig 4E and data not shown). Furthermore, silencing BRCA1 or BRCA2 sensitized ES cells to CP-induced killing (Fig 1C). However, ~70% reduction in ATM or ATR levels did not affect CP-induced loss of viability (Fig 1; Fig 4D) and foci persisted even after CP removal for >24h (Fig 4E). Altogether, this indicates that DSB repair signaling is activated and important, but signal transduction cascades that govern the cellular response to DNA damage beyond repair determine CP-sensitivity.

p53 signaling controls CP-induced apoptosis but not cell cycle arrest in ES cells

Sub-networks were created from molecules enriched in shared canonical pathways from the functional genomics, transcriptomics, and phospho-proteomics datasets (Fig 5). In line with the initiation of ATM signaling an ATM-associated network was found (Fig 5E). A network centered on p53 was also identified (Fig 5A; suppl Table 4). Indeed total protein and active, pSer15-p53 accumulated in a time- and concentration-dependent manner following treatment with CP (Fig 6A). Of 621 p53-regulated genes identified by metacore data-mining software, 100 overlapped with the 2269 CP-regulated genes (Fig 6B,C). Several of these encode pro-apoptotic proteins (Fig 6C genes indicated by *) and in agreement with p53-mediated apoptosis, CP-induced translocation of phosphatidyl-serine to the outer membrane leaflet was p53-dependent (Fig 6D; suppl Fig 1C).

Within the identified differentially expressed p53 target genes, well-known cell cycle regulators were also found (Fig 6C genes indicated by #). For instance, the CDK activator Cdc25c, which is repressed in a p53-dependent manner upon DNA damage (St Clair et al., 2004) was downregulated while Btg2, a p53-responsive antiproliferative BTG family member (Rouault *et al*, 1996) was upregulated. However, since a sublethal dose of 1μM CP induced a G2 arrest that was not affected by p53 silencing (Fig 6E) our data indicate that apoptosis, but not cell cycle arrest is

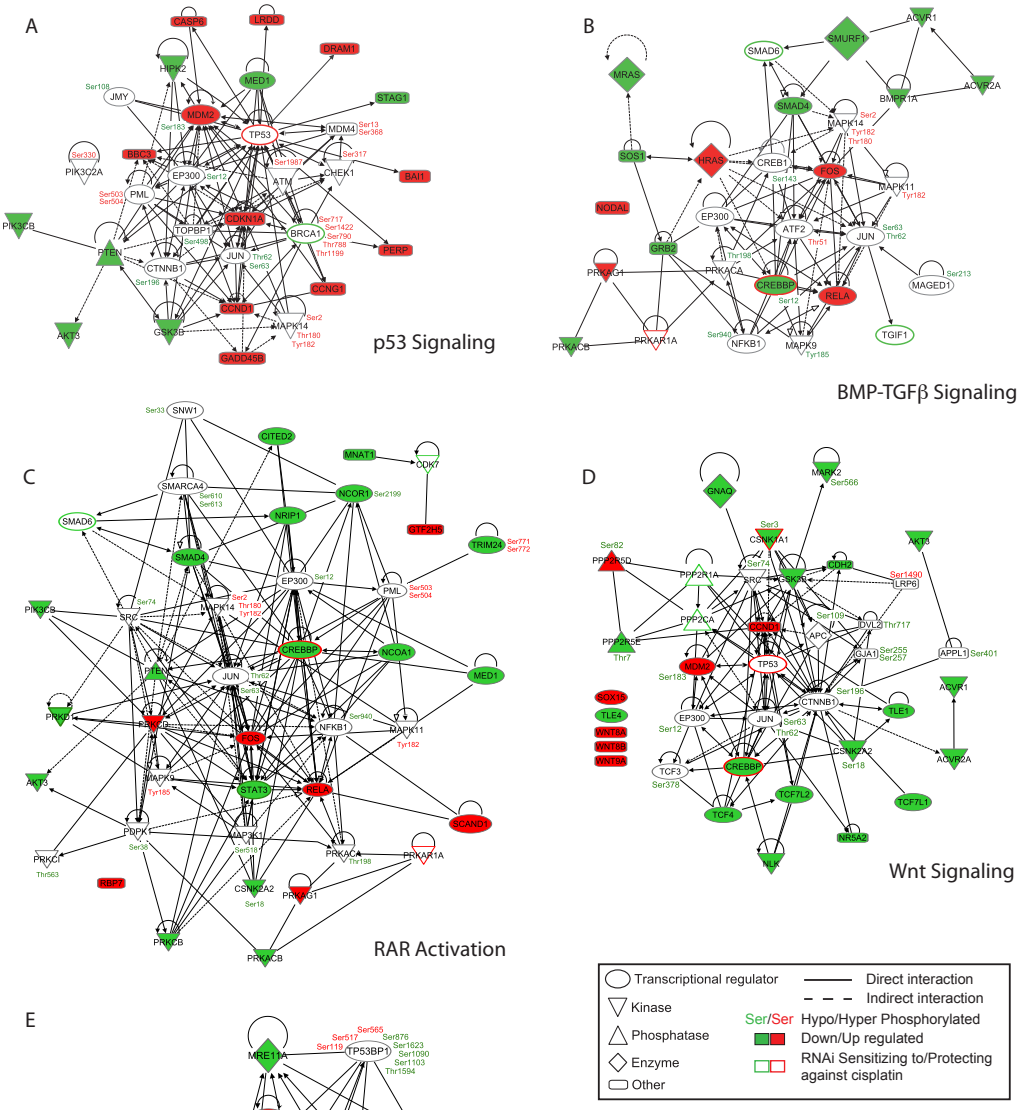

Figure 5. Analysis of interaction-enriched networks of molecules derived from common canonical pathways in the three OMICS data sets. IPA interaction enriched networks of molecules derived from shared canonical pathways in all three datasets p53 signaling **(A)**, TGFβ/ BMP signaling **(B)**, Retinoic Acid Receptor (RAR) activation **(C)**, Wnt signaling **(D)**, and ATM signaling **(E)**. Coding is indicated.

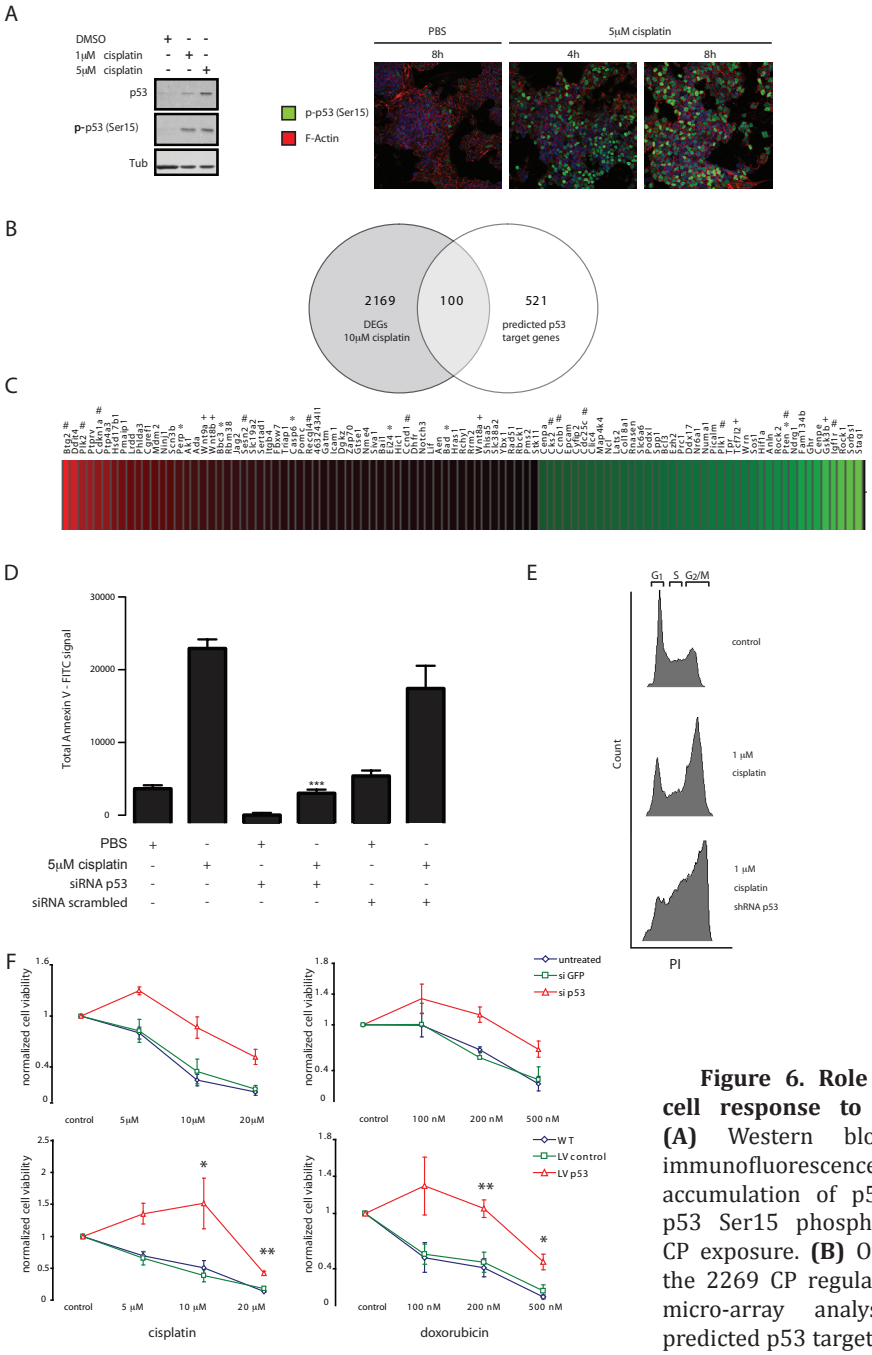

Figure 6. Role of p53 in ES cell response to CP exposure. **(A)** Western blot (left) and immunofluorescence analysis of accumulation of p53 protein and p53 Ser15 phosphorylation upon CP exposure. **(B)** Overlap between the 2269 CP regulated genes from micro-array analysis and 621 predicted p53 target genes obtained using Metacore. **(C)** Ranking of the 100 CP-regulated p53 target genes from B according to level of up- (red) or downregulation (green). Genes previously implicated in apoptosis (*), cell cycle regulation (#) and Wnt (+) are indicated. **(D)** Annexin V-FITC labeling indicates protection against CP-induced apoptosis by si-p53. **(E)** Similar G2/M cell cycle arrest in control and p53-silenced ES cells upon 1μM CP exposure. **(F)** Transient p53 silencing by siRNA (top) and stable lentiviral shRNA p53 silencing (bottom) results in decreased sensitivity to indicated concentrations of CP (left) and doxorubicin (right) whereas control siRNA or shRNA has no effect.

mediated by p53 in ES cells following DNA damage.

Finally, we tested whether the role for p53 in CP-induced apoptosis could be extrapolated to other genotoxic compounds. Indeed, like CP, the response to the topoisomerase inhibitor, doxorubicin was significantly suppressed by synthetic siRNA or lentiviral shRNA targeting p53 (Fig 6F). Altogether, these data strongly support a critical role for p53 in the apoptotic response to genotoxic stress in ES cells.

Differentiation-related signaling networks

Intriguingly, all three datasets predicted differentiation-related networks involved in DDR in ES cells, including "TFGβ signaling", "retinoic acid (RA) receptor (RAR) activation", and "Wnt/β-catenin signaling" (Fig 5). Recently, induction of differentiation has been suggested as an alternative mechanism for stem cells to avoid passage of DNA damage to subsequent cells in the lineage (Sherman *et al*, 2011). However, there was no evidence for ES cell differentiation in response to CP. CP treatment did not alter the expression of key pluripotency markers including Nanog, Oct4, or Sox2 (suppl Fig 2A,B and data not shown) and despite the IPA-predicted "RAR activation" network no overlap between known RA-regulated differentiation genes and identified

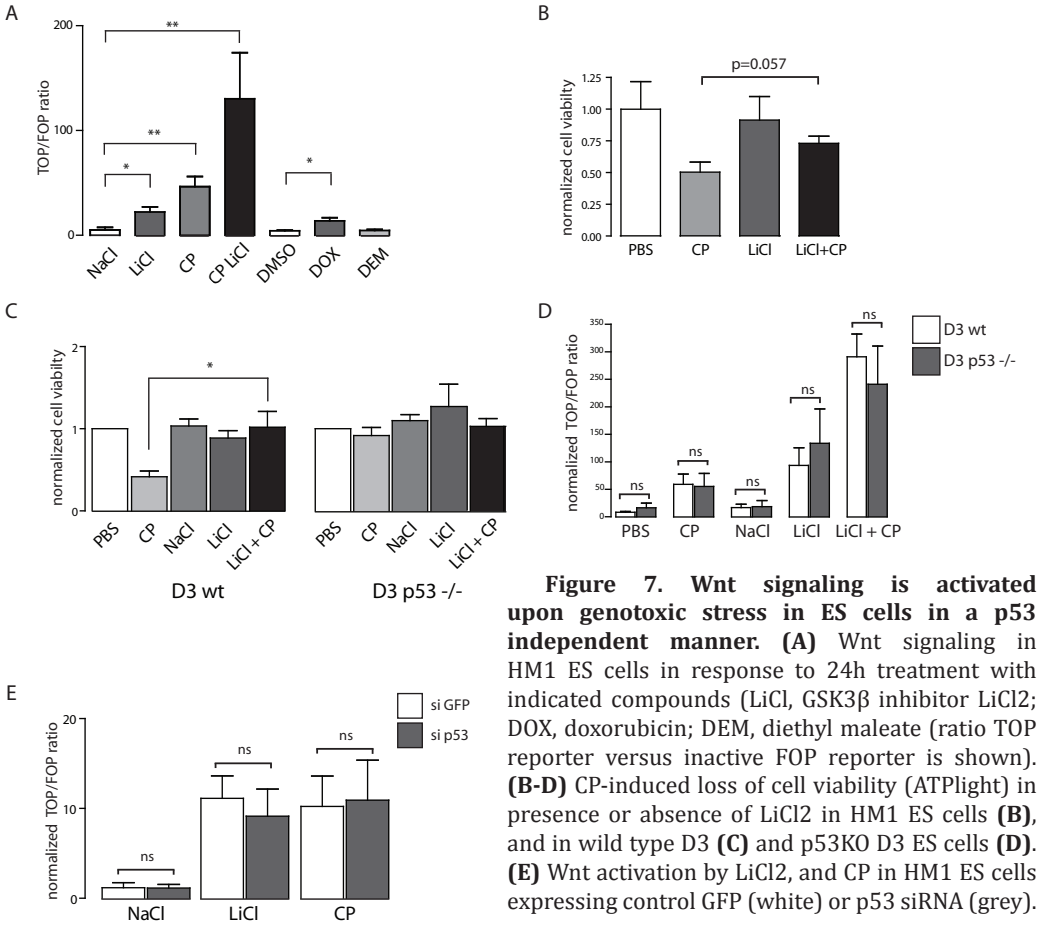

Figure 7. Wnt signaling is activated upon genotoxic stress in ES cells in a p53 independent manner. (A) Wnt signaling in HM1 ES cells in response to 24h treatment with indicated compounds (LiCl, GSK3β inhibitor LiCl2; DOX, doxorubicin; DEM, diethyl maleate (ratio TOP reporter versus inactive FOP reporter is shown). **(B-D)** CP-induced loss of cell viability (ATPlight) in presence or absence of LiCl2 in HM1 ES cells **(B)**, and in wild type D3 **(C)** and p53KO D3 ES cells **(D)**. **(E)** Wnt activation by LiCl2, and CP in HM1 ES cells expressing control GFP (white) or p53 siRNA (grey).

CP-responsive genes was found (suppl Fig 2B). Moreover, our results did not point to differentiation as a protective response: forced differentiation by removal of LIF or addition of RA caused a slight sensitization, rather than protection of ES cells to CP (suppl Fig 2C).

TGFβ / BMP signaling regulates ES cell pluripotency: BMP4 signaling is important for a naïve pluripotent state and TGFβ signaling supports the primed pluripotent state (Hanna *et al*, 2010). Changes in TGFβ signaling predicted by IPA were tested using a TGFβ responsive reporter. ES cells showed basal TGFβ signaling, which, in agreement with the downregulation of the essential co-receptor SMAD4 (Fig 5B), was suppressed by CP (suppl Fig 2D). Exogenous TGFβ could not restore signaling in the presence of CP and, accordingly, did not affect CP sensitivity (suppl Fig 2D,E). The observed downregulation of TGFβ signaling appears to act as a pro-survival response in ES cells, since silencing of the TGFβ-specific inhibitory SMAD6 sensitized ES cells to CP (Fig 1C). Further downregulation of TGFβ signaling using a TGFβR inhibitor did not affect CP sensitivity (suppl Fig 2D,E).

In ES cells, Wnt signaling is important for self-renewal (Berge *et al*, 2011) and p53-mediated upregulation of Wnt ligands has been implicated in genotoxic stress (Lee *et al*, 2010). Wnt reporter induction was observed in response to the genotoxicants CP and doxorubicin but not the oxidative stressor DEM (Fig 7A). Since an available inhibitor of Wnt signaling is known to cross-react with the DNA repair mediator PARP (Karlberg *et al*, 2010), we instead tested if enhanced Wnt signaling could modulate CP sensitivity. The GSK3β inhibitor, $LiCl_2$ synergistically enhanced the induction of Wnt signaling in CP-treated cells and led to decreased CP sensitivity in two different ES cell lines (Fig 7A-D). We tested the reported role for p53 in stress-induced Wnt activity: while deletion or silencing of the *trp53* gene protected against CP-induced loss of viability (Fig 1C; 7C) it did not affect induction of Wnt signaling by CP (Fig 7D,E). Moreover, CP induced Wnt-8a, -8b, and -9a in a p53-dependent manner (Fig 8A,B) as previously described (Lee *et al*, 2010), but silencing these Wnt ligands did not significantly affect survival (Fig 8C). Together, these findings point to an alternative, p53-independent protective role for Wnt-signaling in genotoxic stress in ES cells.

Suppression of negative regulators of Wnt signaling as a protective response to genotoxicity in ES cells

We composed a library of Wnt related genes to identify positive and negative regulators of Wnt signaling in CP-treated ES cells. In agreement with overlapping functionality, silencing of individual members of the Tcf family did not significantly decrease CP-induced Wnt signaling (Fig 8D). Instead, siRNAs targeting the phosphatases PPP2R1a and PPP2ca1 that are implicated in regulating Wnt signaling by dephosphorylation of β Catenin or Axin (Zhang *et al*, 2009; Strovel *et al*, 2000) significantly suppressed CP-induced Wnt activity (Fig 8D). Furthermore, silencing either of two recently identified negative regulators Tcf7l1 (also known as Tcf3; (Yi *et al*, 2011) and CSNK1a1 (Elyada *et al*, 2011) suppressed $LiCl_2$- and CP-induced Wnt activation (Fig 8D). Strikingly, both genes

were downregulated after CP treatment, providing an alternative mechanism for Wnt activation in response to genotoxic stress in ES cells (Fig 8A). We found that CSNK1a1 was downregulated by several genotoxic compounds but not by other stressors tested, including the pro-oxidants menadione and H_2O_2 (Fig 8E,F). Finally, while none of the Tcfs were identified as modulators of CP sensitivity, transient as well as stable lentiviral silencing of CSNK1a1 (but not TCF7L1) protected ES cells against CP-induced killing (Fig1C; 8G,H) without

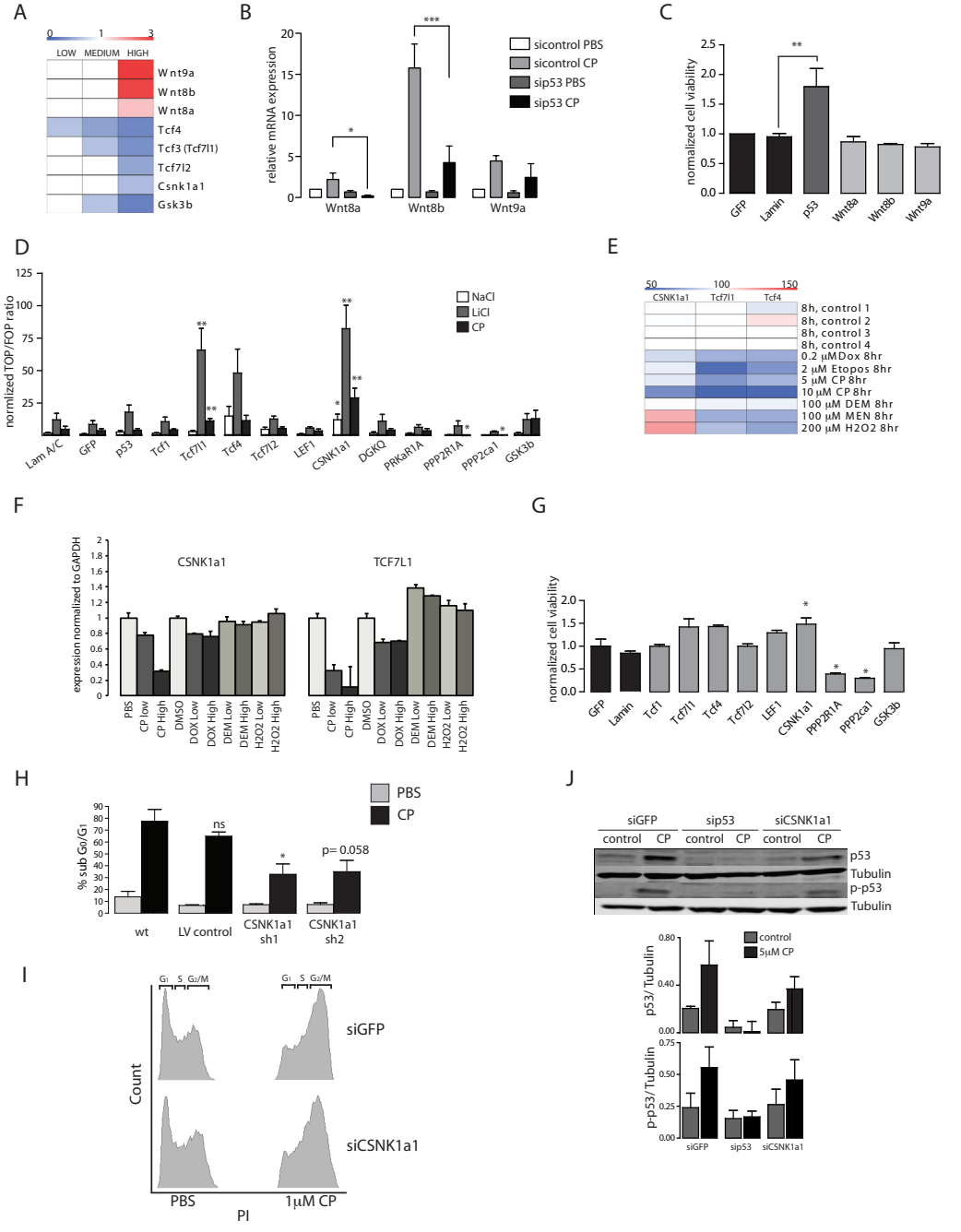

affecting cell cycle progression or p53 levels or activation (Fig8I,J).

Taken together, our findings indicate that genotoxic stress causes marked changes in the relative contributions of pathways involved in self-renewal / pluripotency of ES cells without altering the network of master pluripotency regulators. Our data support a model where the downregulation of CSNK1a1 leads to enhanced Wnt signaling that acts as a brake on p53-mediated apoptosis. It appears that CP triggers a switch from LIF-dependent, Stat3-Myc-mediated self-renewal towards Wnt-mediated control of self-renewal. This would fit the observation that a large number of Stat3- and Myc-controlled genes are downregulated in response to CP (suppl Fig 3), while Wnt signaling is induced. Notably, although Stat3 is downregulated as are several of its downstream targets, Stat3-silencing leads to sensitization; both in ES and 4T1 cells (Fig 1C,G). In ES cells this may reflect the importance of careful tuning of the balance required for self-renewal in ES cells. For both cell types, this may also be due to the important pro-survival signaling mediated by Stat3 for which a threshold level is needed.

ACKNOWLEDGMENTS

We are grateful to Dr. Hoeben, Mr. Rabelink, Dr. ten Dijke, Dr. van de Wetering, and Dr. Willecke for generously providing cells and reagents.

MATERIALS AND METHODS

Cell culture and materials

HM1 mouse ES cells ((Magin *et al*, 1992); provided by Dr. Klaus Willecke, University of Bonn GE) were maintained under feeder free conditions in GMEM medium containing 10% FBS, $5x10^5$ U mouse recombinant leukemia inhibitory factor (LIF; PAA), 25 U/ml penicillin, and 25 μg/ml streptomycin. Wild type and p53 knockout D3 mouse ES cells were cultured in KO-DMEM medium (Invitrogen) with 10% FBS, $5x10^5$ U LIF, and 25 μg/ml streptomycin on feeders. These cells were transferred to gelatinized plates and ES BRL medium (1:1 KO-DMEM and ES BRL conditioned medium) two passages before starting experiments. For RNAi screens and micro-arrays ES cells were used at passage 22 and for all other experiments ES cells were used between passage 20 and 27. 4T1 mouse breast cancer cells

Figure 8. CP-induced downregulation of CSNK1a1 in ES cells mediates Wnt induction suppresses apoptosis. (A) Micro-arrays showing induction of Wnt ligands and suppression of indicated regulators of Wnt signaling in response to low (1μM), medium (5μM), and high (10 μM) CP concentrations. **(B)** qPCR analysis of CP-regulation of expression of Wnt-ligands in HM1 ES cells in absence or presence of si-p53. **(C)** Cell viability in presence of 10 μM CP in ES cells expressing indicated siRNAs. **(D)** Effect of indicated siRNAs on basal (NaCl), or CP- (10μM, 24h) or LiCl2-induced Wnt signaling in ES cells. **(E)** Micro-array analysis of indicated genes in ES cells under control conditions or indicated treatments (dox, doxorobucin; Etopos, Etoposide; DEM, diethyl maleate; MEN, menadione). **(F)** qPCR validation of micro-array shown in E showing analysis of CSNK1a1 and TCF71 expression in ES cells treated with indicated compounds. **(G)** Protection against 10 μM CP-induced killing in ES cells expressing si-CSNK1a1 and sensitization in ES cells expressing siRNAs targeting the phosphatases PPP2R1a and PPP2ca1. **(H)** Stable silencing of CSNK1a1 using shRNAs suppresses CP induced apoptosis (sub G0/G1 fraction analyzed by FACS is shown). **(I)** Silencing CSNK1a1 does not affect basal cell cycle profile or CP-induced G2 arrest in ES cells. **(J)** Silencing CSNK1a1 does not affect p53 protein levels or Ser15 phosphorylation under basal or 5 μM CP-treated conditions.

(ATCC) were cultured in RPMI medium containing 10% FBS and 25 μg/ml streptomycin. All cell lines, including stable shRNA expressing derivatives, were confirmed to be mycoplasma-free using the Mycosensor kit from Stratagene.

Genotoxicants included the DNA cross-linker cisplatin (CP; *Cis*-$PtCl_2(NH_3)_2$) (provided by the Pharmacy unit of University Hospital, Leiden NL) and the inhibitors of topoisomerase II-mediated DNA unwinding, doxorubicin (Sigma) and etoposide (Sigma). Oxidative stressors, included menadione (Sigma), diethyl maleate (Sigma), and H_2O_2 (Merck). The pan-caspase inhibitor z-Val-Ala-DL-Asp-fluoromethylketone (z-VAD-fmk) was purchased from Bachem. SB-431542 TGFβ receptor inhibitor was obtained from Tocris Bioscience. Antibodies against p53 and phospho-p53 were purchased from Novacostra and Cell signaling, respectively. Antibody against Tubulin was obtained from Sigma.

RNAi screening

For primary screens SMARTpool siGENOME libraries targeting all known mouse kinases, phosphatases, and transcription factors were used (ThermoFisher Scientific). For deconvolution confirmation screens, customized libraries containing 4 individual siRNAs targeting each selected mRNA were used (ThermoFisher Scientific). GFP, LaminA/C, and RISC free control siRNAs were used according to MIARE guidelines (Haney, 2007). Kif11 siRNA was used as transfection efficiency control. The siRNA screens were performed on a Biomek FX (Beckman Coulter) liquid handling system. 50nM siRNA was transfected in 96 well plates using Dharmafect1 transfection reagent (ThermoFisher Scientific). The medium was refreshed every 24hr and cells were exposed to indicated compounds or vehicle controls 64h post-transfection for 24h. Primary screens were done in duplicate and deconvolution screens were done in quadruplicate. As readout, a cell viability assay using ATPlite 1Step kit (Perkin Elmer) was performed according to the manufacturer's instructions followed by luminescence measurement using a plate reader. As alternative cell viability readout, Hoechst staining followed by fluorescence reading using a plate reader was performed.

RNAi screen data analysis

As a quality control Z'-factors were determined for each plate, using Lamin A/C as a negative control and p53 as a positive control (Boutros *et al*, 2006). To rank the results, Z-scores were calculated using as a reference i) the mean of all test samples in the primary screen and ii) the mean of the negative control samples in the secondary deconvolution screen (in order to prevent bias due to pre-enrichment of hits) (Birmingham *et al*, 2009). Hit determination was done using Z-scores with a cut off value of 1.5 below or above the reference and p-value lower than 0.05.

Transcriptomics analysis

ES cells were treated with CP (1μM, 5μM or 10μM) or vehicle control for 8h in 3 independent experiments. Total RNA was isolated using the RNAeasy kit (Qiagen) according to manufacturer's instructions. RNA quality and integrity was assessed with Agilent 2100 Bioanalyzer system

(Agilent technologies). Gene expression was measured using Affimetrix MG430 PM Array plates. All raw data passed the affimetrix quality criteria. Normalization of raw data using the robust multi-array average algorithm and statistical analysis was performed using BRBarray tools.

Phosphoproteomics analysis

The experiment analyzing global phosphoproteomics in CP-treated ES cells is published elsewhere and we refer to this for raw data and details on data analysis procedures (Pines *et al*, 2011). In short, SILAC labeling, isolation, and purification of phosphopeptides was performed according to published procedures (Villén *et al*, 2007) and analyzed by tandem Mass Spec.

Integrated data analysis

Pathway and network analysis for hits from functional genomics screens, differentially expressed genes, and differentially phosphorylated proteins were done in Ingenuity Pathway Anaysis (IPA). Canonical pathways were grouped according to Ingenuity pathway classification. Analysis of transcription factor targets was done using MetaCore data-mining software. Outgoing interactions from p53, as well as downstream interactions from Stat3, and c-Myc transcription factors, were checked for overlap with significantly regulated genes from the microarray dataset.

Apoptosis and cell cycle analysis

Floating and attached cells were pooled and fixed in 80% ethanol overnight. Cells were stained using PBS EDTA containing 7.5mM propidium iodine and 40mg/ml RNAseA and measured by flow cytometry (FACSCanto II; Becton Dickinson). The amount of cells in the different cell cycle fractions (and in sub G0/G1 for apoptotic cells) was calculated using the BD FACSDiva software. As an alternative method to determine apoptosis, phosphatidyl-serine exposure at the outer membrane leaflet was detected by Annexin V-FITC in real-time in attached cells as described previously (Puigvert *et al*, 2010).

Western blot analysis

Total extracts were prepared in SDS protein lysis sample buffer and boiled for 5 min at 95°C. Extracts were separated by SDS-PAGE on polyacrylamide gels, transferred to PVDF membranes, and membranes were blocked using 5% BSA. Following incubation with primary and secondary antibodies signal was detected using a Typhoon™ 9400 from GE Healthcare.

Immunofluorescence

Cells were plated in μClear 96 well/ plates (GREINER) coated with 1% gelatin and exposed to vehicle (PBS) or 5μM CP for 4h and 8h. Fixation of the samples was done using 4% paraformaldehyde following incubation with primary and secondary antibodies and images were captured using a Nikon TE2000 EPI microscope.

Stable p53 & CSNK1a1 silencing

Cells were transduced using lentiviral TRC shRNA vectors at MOI 1 (LentiExpressTM; Sigma-Aldrich; Dr. R. Hoeben and M. Rabelink, University Hospital, Leiden NL) according to the manufacturers' procedures and selected in medium containing 1 μg/ml puromycin. Control vector expressed

shRNA targeting TurboGFP and 2 independent shRNAs silencing mouse p53 or CSNK1a1 genes were selected from set of 5 based on most efficient silencing in bulk puromycin-selected cells.

qPCR

RNA was extracted using RNeasy Plus Mini Kit from Qiagen. cDNA was made from 50 ng total RNA with RevertAid H minus First strand cDNA synthesis kit (Fermentas) and real-time qPCR was subsequently performed in triplicate using SYBR green PCR (Applied Biosystems) on a 7900HT fast real-time PCR system (Applied Biosystems). The following qPCR primer sets were used: GAPDH, forward (fw) *tccatgacaactttggcattg* reverse (rev) *tcacgccacagctttcca*; ATM, fw *aacaaagtcttagtgatactgaccagagttt* rev *cacgctcagctactttgttgaaa*; ATR, fw *tgaaggacatgtgcattacctcata* rev *accaaggtacatctgacagagtaagttt*; WNT8a, fw *taaccggtcccaaggccta*, rev *gccgcagttttccaagtcac*; WNT8b, fw *ataccagtttgcttgggaccg*, rev *cgaagcccacgttgtcact*; WNT9a, fw *gggtccagaagacccagactt*, rev *tctgtggtggtcgtgtgactg*; CSNK1a1, fw *cctccatcttcgcgtctcag*, rev *accgtatgtgagggatgcca*; TCF7L1, forward *ccctgcagtgagtgcgaaat*, reverse *gtagagctgcgcgtgaagc*. Data were collected and analyzed using SDS2.3 software (Applied Biosystems). Relative mRNA levels after correction for GAPDH control mRNA were expressed using 2^(-ΔΔCt) method.

Wnt & TGFβ reporter assays

For Wnt signal analysis, cells were transiently transfected with 20 ng pGL4-Top5 firefly luciferase reporter plasmid containing 5 TCF-responsive elements and a minimal TATA box or a pGL4-Fop5 control plasmid in which TCF-responsive elements were mutated (Smit *et al*, 2004) (provided by Dr. M. van de Wetering, Hubrecht Institute, Utrecht NL) using Lipofectamine 2000. For TGFβ signal analysis, a (CAGA)12 firefly luciferase reporter was used (Dennler *et al*, 1998) (provided by Dr. P. ten Dijke, University Hospital, Leiden NL). Reporter activity was analyzed using a luciferase assay kit (Promega) 72h post transfection according to the manufacturers' procedure.

REFERENCES

Aladjem MI, Spike BT, Rodewald LW, Hope TJ, Klemm M, Jaenisch R & Wahl GM (1998) ES cells do not activate p53-dependent stress responses and undergo p53-independent apoptosis in response to DNA damage. *Current biology : CB* **8:** 145-55

Arora S, Bisanz KM, Peralta L a, Basu GD, Choudhary A, Tibes R & Azorsa DO (2010) RNAi screening of the kinome identifies modulators of cisplatin response in ovarian cancer cells. *Gynecologic Oncology* **118:** 220-227

Bartek J, Bartkova J & Lukas J (2007) DNA damage signalling guards against activated oncogenes and tumour progression. *Oncogene* **26:** 7773-9

Berge DT, Kurek D, Blauwkamp T, Koole W, Maas A, Eroglu E, Siu RK & Nusse R (2011) Embryonic stem cells require Wnt proteins to prevent differentiation to epiblast stem cells. *Nature Cell Biology* **13:** 1070-1075

Birmingham A, Selfors LM, Forster T, Wrobel D, Kennedy CJ, Shanks E, Santoyo-Lopez J, Dunican DJ, Long A, Kelleher D, Smith Q, Beijersbergen RL, Ghazal P & Shamu CE (2009) Statistical methods for analysis of high-throughput RNA interference screens. *Nature Methods* **6:** 569-575

Blanpain C, Mohrin M, Sotiropoulou P a & Passegué E (2011) DNA-Damage Response in

Tissue-Specific and Cancer Stem Cells. *Cell Stem Cell* **8:** 16-29

Boutros M, Brás LP & Huber W (2006) Analysis of cell-based RNAi screens. *Genome biology* **7:** R66

Ciccia A & Elledge SJ (2010) The DNA Damage Response: Making It Safe to Play with Knives. *Molecular Cell* **40:** 179-204

Cortez D, Guntuku S, Qin J & Elledge SJ (2001) ATR and ATRIP: partners in checkpoint signaling. *Science (New York, N.Y.)* **294:** 1713-6

Dennler S, Itoh S, Vivien D, ten Dijke P, Huet S & Gauthier JM (1998) Direct binding of Smad3 and Smad4 to critical TGF beta-inducible elements in the promoter of human plasminogen activator inhibitor-type 1 gene. *The EMBO journal* **17:** 3091-100

Elyada E, Pribluda A, Goldstein RE, Morgenstern Y, Brachya G, Cojocaru G, Snir-Alkalay I, Burstain I, Haffner-Krausz R, Jung S, Wiener Z, Alitalo K, Oren M, Pikarsky E & Ben-Neriah Y (2011) CKIα ablation highlights a critical role for p53 in invasiveness control. *Nature* **470:** 409-413

Hakem R (2008) DNA-damage repair; the good, the bad, and the ugly. *The EMBO journal* **27:** 589-605

Hamid R & Brandt SJ (2009) Transforming growth-interacting factor (TGIF) regulates proliferation and differentiation of human myeloid leukemia cells. *Molecular oncology* **3:** 451-63

Haney S a (2007) Increasing the robustness and validity of RNAi screens. *Pharmacogenomics* **8:** 1037-49

Hanna JH, Saha K & Jaenisch R (2010) Pluripotency and Cellular Reprogramming: Facts, Hypotheses, Unresolved Issues. *Cell* **143:** 508-525

Harper JW & Elledge SJ (2007) The DNA damage response: ten years after. *Molecular cell* **28:** 739-45

Hoeijmakers JHJ (2009) DNA damage, aging, and cancer. *The New England journal of medicine* **361:** 1475-85

Huang R, Wu T, Xu L, Liu A, Ji Y & Hu G (2002) Upstream binding factor up-regulated in hepatocellular carcinoma is related to the survival and cisplatin-sensitivity of cancer cells. *The FASEB journal : official publication of the Federation of American Societies for Experimental Biology* **16:** 293-301

Jackson SP & Bartek J (2009) The DNA-damage response in human biology and disease. *Nature* **461:** 1071-8

Jing N & Tweardy DJ (2005) Targeting Stat3 in cancer therapy. *Anti-cancer drugs* **16:** 601-7

Jordan P & Carmo-Fonseca M (2000) Molecular mechanisms involved in cisplatin cytotoxicity. *Cellular and Molecular Life Sciences* **57:** 1229-1235

Karlberg T, Markova N, Johansson I, Hammarström M, Schütz P, Weigelt J & Schüler H (2010) Structural basis for the interaction between tankyrase-2 and a potent Wnt-signaling inhibitor. *Journal of medicinal chemistry* **53:** 5352-5

Kodama M, Otsubo C, Hirota T, Yokota J, Enari M & Taya Y (2010) Requirement of ATM for rapid p53 phosphorylation at Ser46 without Ser/Thr-Gln sequences. *Molecular and cellular biology* **30:** 1620-33

Kolas NK, Chapman JR, Nakada S, Ylanko J, Chahwan R, Sweeney FD, Panier S, Mendez M, Wildenhain J, Thomson TM, Pelletier L, Jackson SP & Durocher D (2007) Orchestration of the DNA-damage response by the RNF8 ubiquitin ligase. *Science (New York, N.Y.)* **318:** 1637-40

Lee K-H, Li M, Michalowski AM, Zhang X, Liao H, Chen L, Xu Y, Wu X & Huang J (2010) A genomewide study identifies the Wnt signaling pathway as a major target of p53 in murine embryonic stem cells. *Proceedings of the National Academy of Sciences of the United States of America* **107:** 69-74

Lin T, Chao C, Saito S, Mazur SJ, Murphy ME, Appella E & Xu Y (2005) p53 induces differentiation of mouse embryonic stem cells by suppressing Nanog expression. *Nature cell biology* **7:** 165-71

Liu F (2008) PCTA: a new player in TGF-beta signaling. *Science signaling* **1:** pe49

Lombard DB, Chua KF, Mostoslavsky R, Franco S, Gostissa M & Alt FW (2005) DNA repair, genome stability, and aging. *Cell* **120:** 497-512

MacKeigan JP, Murphy LO & Blenis J (2005) Sensitized RNAi screen of human kinases and phosphatases identifies new regulators of apoptosis and chemoresistance. *Nature cell biology* **7:** 591-600

Magin TM, McWhir J & Melton DW (1992) A new mouse embryonic stem cell line with good germ line contribution and gene targeting frequency. *Nucleic acids research* **20:** 3795-6

Matsuoka S, Ballif B a, Smogorzewska A, McDonald ER, Hurov KE, Luo J, Bakalarski CE, Zhao Z, Solimini N, Lerenthal Y, Shiloh Y, Gygi SP & Elledge SJ (2007) ATM and ATR substrate analysis reveals extensive protein networks responsive to DNA damage. *Science (New York,*

N.Y.) **316:** 1160-6

Naderi EH, Findley HW, Ruud E, Blomhoff HK & Naderi S (2009) Activation of cAMP signaling inhibits DNA damage-induced apoptosis in BCP-ALL cells through abrogation of p53 accumulation. *Blood* **114:** 608-18

Orlov SN, Thorin-Trescases N, Dulin NO, Dam TV, Fortuno M a, Tremblay J & Hamet P (1999) Activation of cAMP signaling transiently inhibits apoptosis in vascular smooth muscle cells in a site upstream of caspase-3. *Cell death and differentiation* **6:** 661-72

Panayiotou C, Solaroli N, Xu Y, Johansson M & Karlsson A (2011) The characterization of human adenylate kinases 7 and 8 demonstrates differences in kinetic parameters and structural organization among the family of adenylate kinase isoenzymes. *The Biochemical journal* **433:** 527-34

Parrilla-Castellar ER, Arlander SJH & Karnitz L (2004) Dial 9-1-1 for DNA damage: the Rad9-Hus1-Rad1 (9-1-1) clamp complex. *DNA repair* **3:** 1009-14

Paulsen RD, Soni DV, Wollman R, Hahn AT, Yee M-C, Guan A, Hesley J a, Miller SC, Cromwell EF, Solow-Cordero DE, Meyer T & Cimprich K a (2009) A genome-wide siRNA screen reveals diverse cellular processes and pathways that mediate genome stability. *Molecular cell* **35:** 228-39

Pines A, Kelstrup CD, Vrouwe MG, Puigvert JC, Typas D, Misovic B, de Groot A, von Stechow L, van de Water B, Danen EHJ, Mullenders LHF & Olsen JV (2011) Global phosphoproteome profiling reveals unanticipated networks responsive to cisplatin treatment of embryonic stem cells . *submitted*

Polo SE & Jackson SP (2011) Dynamics of DNA damage response proteins at DNA breaks: a focus on protein modifications. *Genes & Development* **25:** 409-433

Puigvert JC, de Bont H, van de Water B & Danen EHJ (2010) High-throughput live cell imaging of apoptosis. *Current protocols in cell biology* **Chapter 18:** Unit 18.10.1-13

Rouault JP, Falette N, Guéhenneux F, Guillot C, Rimokh R, Wang Q, Berthet C, Moyret-Lalle C, Savatier P, Pain B, Shaw P, Berger R, Samarut J, Magaud JP, Ozturk M, Samarut C & Puisieux A (1996) Identification of BTG2, an antiproliferative p53-dependent component of the DNA damage cellular response pathway. *Nature genetics* **14:** 482-6

Räschle M, Knipscheer P, Enoiu M, Angelov T, Sun J, Griffith JD, Ellenberger TE, Schärer OD & Walter JC (2008) Mechanism of replication-coupled DNA interstrand crosslink repair. *Cell* **134:** 969-80

Sabapathy K, Klemm M, Jaenisch R & Wagner EF (1997) Regulation of ES cell differentiation by functional and conformational modulation of p53. *The EMBO journal* **16:** 6217-29

Sherman MH, Bassing CH & Teitell M a (2011) Regulation of cell differentiation by the DNA damage response. *Trends in cell biology* **21:** 312-9

Smit L, Baas A, Kuipers J, Korswagen H, van de Wetering M & Clevers H (2004) Wnt activates the Tak1/Nemo-like kinase pathway. *The Journal of biological chemistry* **279:** 17232-40

Solozobova V, Rolletschek A & Blattner C (2009) Nuclear accumulation and activation of p53 in embryonic stem cells after DNA damage. *BMC cell biology* **10:** 46

Strovel ET, Wu D & Sussman DJ (2000) Protein phosphatase 2Calpha dephosphorylates axin and activates LEF-1-dependent transcription. *The Journal of biological chemistry* **275:** 2399-403

Villén J, Beausoleil SA, Gerber SA & Gygi SP (2007) Large-scale phosphorylation analysis of mouse liver. *Proceedings of the National Academy of Sciences of the United States of America* **104:** 1488-93

Yang C, Hornicek FJ, Wood KB, Schwab JH, Choy E, Mankin H & Duan Z (2010) Blockage of Stat3 with CDDO-Me inhibits tumor cell growth in chordoma. *Spine* **35:** 1668-75

Yi F, Pereira L, Hoffman J a, Shy BR, Yuen CM, Liu DR & Merrill BJ (2011) Opposing effects of Tcf3 and Tcf1 control Wnt stimulation of embryonic stem cell self-renewal. *Nature cell biology* **13:** 762-70

Zhang W, Yang J, Liu Y, Chen X, Yu T, Jia J & Liu C (2009) PR55 alpha, a regulatory subunit of PP2A, specifically regulates PP2A-mediated beta-catenin dephosphorylation. *The Journal of biological chemistry* **284:** 22649-56

Zou L & Elledge SJ (2003) Sensing DNA damage through ATRIP recognition of RPA-ssDNA complexes. *Science (New York, N.Y.)* **300:** 1542-8

SUPPLEMENTAL DATA

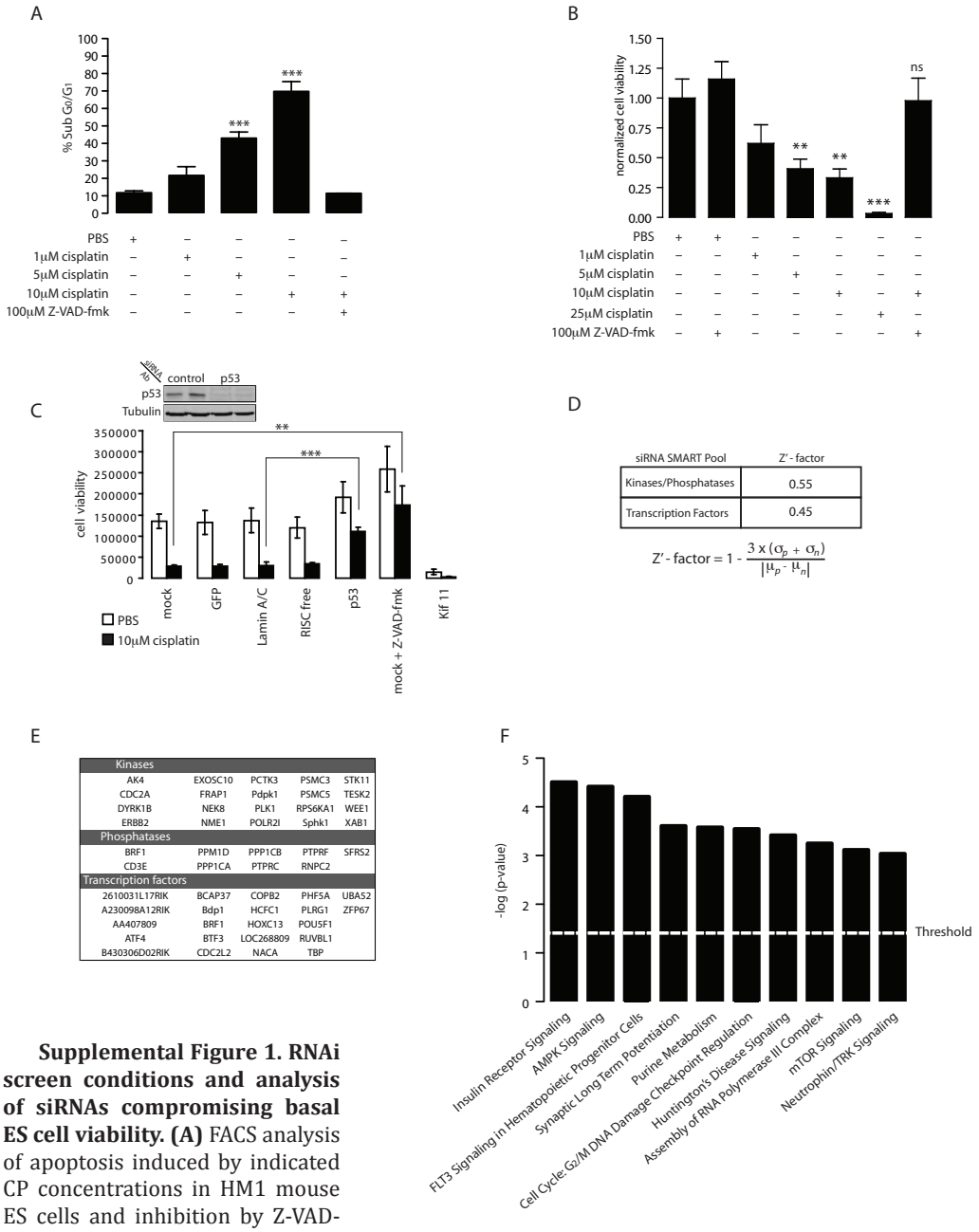

Supplemental Figure 1. RNAi screen conditions and analysis of siRNAs compromising basal ES cell viability. (A) FACS analysis of apoptosis induced by indicated CP concentrations in HM1 mouse ES cells and inhibition by Z-VAD-fmk. **(B)** ATPlight analysis of loss-of viability induced by indicated CP concentrations in HM1 mouse ES cells and inhibition by Z-VAD-fmk. **(C)** Western blot shows efficient silencing of p53 using si-p53 but not control siRNA. Graph shows protection against CP-induced loss of viability by si-p53 and Z-VAD-fmk and killing under basal and CP-conditions by si-Kif11. **(D)** Average Z'factor calculated for all plates under CP-treated conditions from screens including indicated gene families. **(E)** siRNA SMARTpools targeting indicated genes that conferred significant loss of viability under control conditions, which were excluded from further analysis. **(F)** Overrepresented canonical pathways obtained using IPA from interaction-enriched networks derived from genes in E.

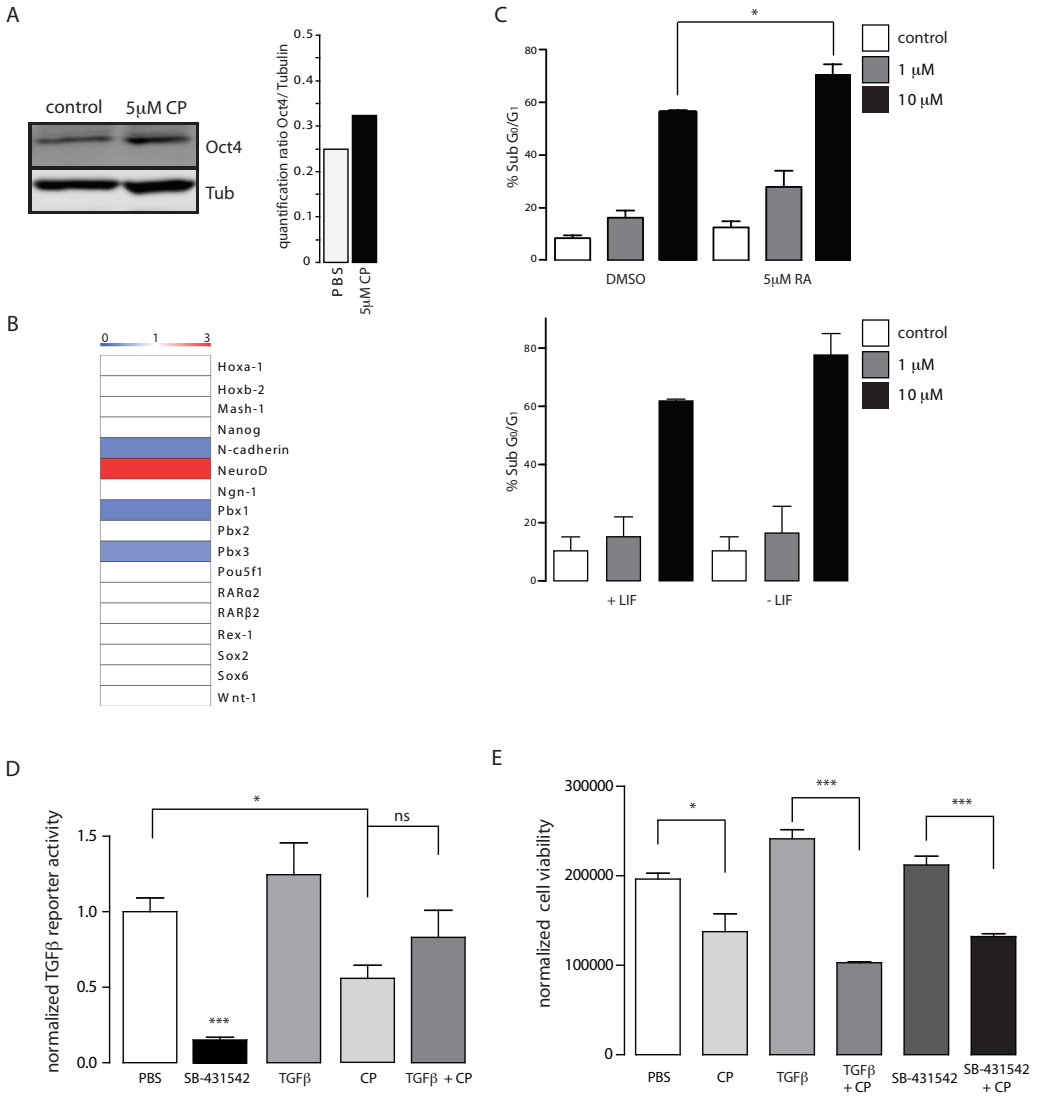

Supplemental Figure 2. TGFβ and RA modulation of response to CP. (A) Western blot analysis of Oct4 protein levels under control and CP conditions. Graph shows quantification of Western blot results. **(B)** Micro-array showing general lack of response to CP treatment for known RA target genes and pluripotency markers, Pou5f1, Sox2 and Nanog. **(C)** FACS analysis of apoptosis in HM1 cells induced by indicated CP concentrations in absence or presence of RA (5 μM 48 pre-CP; top) or LIF (48h withdrawal pre-CP; bottom) **(D)** TGFβ reporter activity in HM1 cells treated with indicated compounds (CP 10 μM; SB-431542 10 nM; TGFβ 10 nM). **(E)** Cell viability (ATPlight) for HM1 cells treated with indicated compounds as in D.

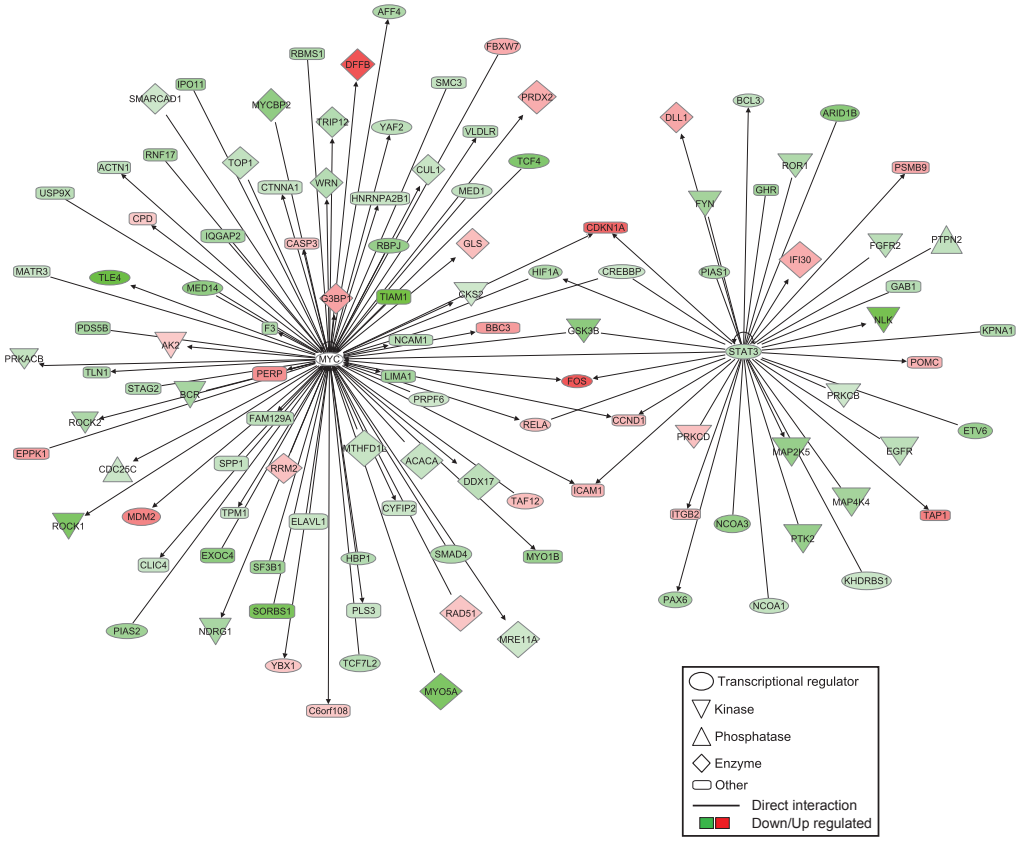

Supplemental Figure 3. Stat3 and cMyc downstream interacting molecules transcriptionally downregulated upon CP exposure. IPA network of molecules derived from overlap between the transcriptomics data set and known downstream molecules from Stat3 and cMyc. Red indicates upregulation; green indicates downregulation.

Supplemental Table 1: siRNAs protecting against or sentizing to cisplatin in ES cells identified in primary SMARTpool screen and confirmation in secondary deconvolution screen.

A: siRNAs protecting against cisplatin

Gene symbol	Gene Name Aliases	Protein ID	Activity	Confirmation
NCOA3	Nuclear receptor coactivator 3	O09000	Acetyltransferase	1 out of 4
CREBBP	CREB-binding protein	P45481	Acetyltransferase	3 out of 4
CALR	Calreticulin	P14211	Calcium-binding Protein	2 out of 4
CRY1	Cryptochrome-1	P97784	DNA Photolyase	1 out of 4
ADCK4	Uncharacterized aarF domain-containing protein kinase 4	Q566J8	Hydrolase	1 out of 4
Trpm7	Transient receptor potential cation channel subfamily M member 7	Q923J1	Ion Channel	4 out of 4
LIMK2	LIM domain kinase 2	O54785	Kinase	1 out of 4
EGFR	Epidermal growth factor receptor	Q01279	Kinase	1 out of 4
CDC2L5	Cell division cycle 2-like protein kinase 5	Q69ZA1	Kinase	1 out of 4
RET	Proto-oncogene tyrosine-protein kinase receptor ret	P35546	Kinase	1 out of 4
NME6	Nucleoside diphosphate kinase 6	O88425	Kinase	1 out of 4
NME7	Nucleoside diphosphate kinase 7	Q9QXL8	Kinase	1 out of 4
RPS6KA2	Ribosomal protein S6 kinase alpha-2	Q9WUT3	Kinase	1 out of 4
RAGE	MAPK/MAK/MRK overlapping kinase	Q9WVS4	Kinase	1 out of 4
ROCK2	Rho-associated protein kinase 2	P70336	Kinase	1 out of 4
Lmtk2	Serine/threonine-protein kinase LMTK2	Q3TYD6	Kinase	1 out of 4
PRKCB	Protein kinase C beta type	P68404	Kinase	1 out of 4
PDGFRB	Beta-type platelet-derived growth factor receptor	P05622	Kinase	1 out of 4
TEC	Tyrosine-protein kinase Tec	P24604	Kinase	1 out of 4
CSNK1G1	Casein kinase I isoform gamma-1	Q8BTH8	Kinase	1 out of 4
DAPK1	Death-associated protein kinase 1	Q80YE7	Kinase	1 out of 4
AKAP4	A-kinase anchor protein 4	Q60662	Kinase	2 out of 4
NEK6	Serine/threonine-protein kinase Nek6	Q9ES70	Kinase	2 out of 4
CSNK1G2	Casein kinase I isoform gamma-2	Q8BVP5	Kinase	2 out of 4
AK3L	GTP:AMP phosphotransferase mitochondrial	Q9WTP7	Kinase	2 out of 4
Bmp2k	BMP-2-inducible protein kinase	Q91Z96	Kinase	2 out of 4
GALK1	Galactokinase	Q9R0N0	Kinase	2 out of 4
LTK	Leukocyte tyrosine kinase receptor	P08923	Kinase	3 out of 4
CSNK1A1	Casein kinase I isoform alpha	Q8BK63	Kinase	3 out of 4
PRKAR1A	cAMP-dependent protein kinase type I-alpha regulatory subunit	Q9DBC7	Kinase	4 out of 4
RIPK3	Receptor-interacting serine/threonine-protein kinase 3	Q9QZL0	Kinase	2 out of 4
NRBP	Nuclear receptor-binding protein	Q99J45	Kinase	2 out of 4
CDKN2C	Cyclin-dependent kinase 4 inhibitor C	Q60772	Kinase Inhibitor	1 out of 4
SITPEC	Evolutionarily conserved signaling intermediate in Toll pathway	Q9QZH6	Kinase Modulator	1 out of 4
D11BWG0280E	Zinc finger MIZ domain-containing protein 2	Q8CIE2	Ligase Activity	1 out of 4
PUS1	tRNA pseudouridine synthase A	Q9WU56	Lyase	1 out of 4
DUSP12	Dual specificity protein phosphatase 12	Q9D0T2	Phosphatase	1 out of 4
PSPH	Phosphoserine phosphatase	Q99LS3	Phosphatase	1 out of 4
PPAP2A	Lipid phosphate phosphohydrolase 1	Q61469	Phosphatase	3 out of 4
PPM1L	Protein phosphatase 1L	Q8BHN0	Phosphatase	1 out of 4
CDKN3	Cdkn3	Q810P3	Phosphatase	1 out of 4
DUSP19	Dual specificity protein phosphatase 19	Q8K4T5	Phosphatase	1 out of 4
PPM1G	Protein phosphatase 1G	Q61074	Phosphatase	2 out of 4
MTM1	Myotubularin	Q9Z2C5	Phosphatase	1 out of 4
DUSP15	Dual specificity protein phosphatase 15	Q8R4V2	Phosphatase	3 out of 4
BPNT1	3'(2'),5'-bisphosphate nucleotidase 1	Q9Z0S1	Phosphatase	1 out of 4
MRC2	C-type mannose receptor 2	Q64449	Receptor Activity	1 out of 4
HDAC2	Histone deacetylase 2	P70288	Reductase	1 out of 4
IRX3	Iroquois-class homeodomain protein IRX-3	P81067	Transcription Regulation	1 out of 4
GATA1	Erythroid transcription factor	P17679	Transcription Regulation	1 out of 4
GAS7	Growth arrest-specific protein 7	Q60780	Transcription Regulation	1 out of 4
GCM1	Chorion-specific transcription factor GCMa	P70348	Transcription Regulation	1 out of 4
EGR2	Early growth response protein 2	P08152	Transcription Regulation	1 out of 4
MYBL2	Myb-related protein B	P48972	Transcription Regulation	1 out of 4
TCFCP2L3	Grainyhead-like protein 2 homolog	Q8K5C0	Transcription Regulation	1 out of 4
IRF5	Interferon regulatory factor 5	P56477	Transcription Regulation	1 out of 4
Mterf	Transcription termination factor, mitochondrial	Q8CHZ9	Transcription Regulation	1 out of 4
FOXE3	Forkhead box protein E3	Q9QY14	Transcription Regulation	1 out of 4
MAFF	Transcription factor MafF	O54791	Transcription Regulation	1 out of 4
GTF3A	Transcription factor IIIA	Q8VHT7	Transcription Regulation	1 out of 4
IDB3	DNA-binding protein inhibitor ID-3	P41133	Transcription Regulation	1 out of 4
MAZ	Myc-associated zinc finger protein	P56671	Transcription Regulation	1 out of 4
CEBPB	CCAAT/enhancer-binding protein beta	P28033	Transcription Regulation	1 out of 4
TRIM25	Tripartite motif-containing protein 25	Q61510	Transcription Regulation	1 out of 4
HOXC8	Homeobox protein Hox-C8	P09025	Transcription Regulation	1 out of 4
TCFL4	Max-like protein X	O08609	Transcription Regulation	1 out of 4
TFDP1	Transcription factor Dp-1	Q08639	Transcription Regulation	1 out of 4
VAV1	Proto-oncogene vav	P27870	Transcription Regulation	1 out of 4
JUNDM2	Jun dimerization protein 2	P97875	Transcription Regulation	1 out of 4
NEUROD2	Neurogenic differentiation factor 2	Q62414	Transcription Regulation	1 out of 4
FOXP4	Forkhead box protein P4	Q9DBY0	Transcription Regulation	1 out of 4
CITED2	Cbp/p300-interacting transactivator 2	O35740	Transcription Regulation	2 out of 4
ARX	Homeobox protein ARX	O35085	Transcription Regulation	2 out of 4
TCFE2A	Transcription factor E2-alpha	P15806	Transcription Regulation	2 out of 4
MYB	Myb proto-oncogene protein	P06876	Transcription Regulation	2 out of 4
IRF2	Interferon regulatory factor 2	P23906	Transcription Regulation	2 out of 4
SMAD1	Mothers against decapentaplegic homolog 1	P70340	Transcription Regulation	2 out of 4
ZFP29	Zinc finger and SCAN domain-containing protein 2	Q07230	Transcription Regulation	2 out of 4
ATF7	Cyclic AMP-dependent transcription factor ATF-7	Q8R0S1	Transcription Regulation	3 out of 4
Trp53	Cellular tumor antigen p53	P02340	Transcription Regulation	4 out of 4
FEV	Protein FEV	Q8QZW2	Transcription Regulation	1 out of 4
Maf	Transcription factor Maf	P54843	Transcription Regulation	1 out of 4
MECP2	Methyl-CpG-binding protein 2	Q9Z2D6	Transcription Regulation	1 out of 4
TEX14	Testis-expressed protein 14	Q7M6U3		1 out of 4
1200013B22RIK				2 out of 4
FUK				2 out of 4
DGKQ				2 out of 4
CARD14	Caspase recruitment domain-containing protein 14	Q99KF0		2 out of 4
1700011K15RIK				2 out of 4
PTPRB				1 out of 4
PTPRU				1 out of 4
2410018C20RIK				1 out of 4
RFX5				1 out of 4
IFI16				1 out of 4
Hdh	Huntingtin	P42859		1 out of 4
SMARCA2				1 out of 4
HOD	Homeodomain-only protein	Q8R1H0		1 out of 4
LOC433182				1 out of 4
AXUD1	Axin-1 up-regulated gene 1 protein	P59054		2 out of 4
EP300				2 out of 4
4921511I16RIK				2 out of 4
SS18L1				2 out of 4
2610014H22RIK				3 out of 4
6430502M16RIK				3 out of 4
ASB4	Ankyrin repeat and SOCS box protein 4	Q9WV71		3 out of 4

B: siRNAs sensitizing to cisplatin

Gene symbol	Gene Name Aliases	Protein ID	Activity	Confirmation
PLK2	Serine/threonine-protein kinase PLK2	P53351	Kinase	1 out of 4
CCRK	Cell cycle-related kinase	Q9JHU3	Kinase	2 out of 4
AMHR2	Anti-Muellerian hormone type-2 receptor	Q8K592	Kinase	2 out of 4
FLT3	FL cytokine receptor	Q00342	Kinase	2 out of 4
AURKB	Serine/threonine-protein kinase 12	O70126	Kinase	2 out of 4
PRKCN	Serine/threonine-protein kinase D3	Q8K1Y2	Kinase	2 out of 4
HUNK	Hormonally up-regulated neu tumor-associated kinase	Q88866	Kinase	2 out of 4
TESK2	Dual specificity testis-specific protein kinase 2	Q8VCT9	Kinase	2 out of 4
PCTK1	Serine/threonine-protein kinase PCTAIRE-1	Q04735	Kinase	3 out of 4
PRKCM	Serine/threonine-protein kinase D1	Q62101	Kinase	3 out of 4
STK6	Serine/threonine-protein kinase 6	P97477	Kinase	3 out of 4
CDK7	Cell division protein kinase 7	Q03147	Kinase	3 out of 4
JAK1	Tyrosine-protein kinase JAK1	P52332	Kinase	3 out of 4
STK10	Serine/threonine-protein kinase 10	O55098	Kinase	3 out of 4
HK3	Hexokinase-3	Q3TRM8	Kinase	3 out of 4
PIK4CB	Phosphatidylinositol 4-kinase beta	Q8BKC8	Kinase	4 out of 4
EPHB2	Ephrin type-B receptor 2	P54763	Kinase	4 out of 4
DYRK3	Dual specificity tyrosine-phosphorylation-regulated kinase 3	Q922Y0	Kinase	4 out of 4
MET	Hepatocyte growth factor receptor	P16056	Kinase	4 out of 4
PRPF4B	Serine/threonine-protein kinase PRP4 homolog	Q61136	Kinase	4 out of 4
CDK7	Cell division protein kinase 7	Q03147	Kinase	3 out of 4
DMAP1	DNA methyltransferase 1-associated protein 1	Q9JI44	Methyltransferase	3 out of 4
HNF4	Hepatocyte nuclear factor 4-alpha	P49698	Nuclear Hormone Receptor	2 out of 4
Dusp1	Dual specificity protein phosphatase 1	P28563	Phosphatase	2 out of 4
Dusp1	Dual specificity protein phosphatase 1	P28563	Phosphatase	2 out of 4
PPP1R1B	Protein phosphatase 1 regulatory subunit 1B	Q60829	Phosphatase	2 out of 4
MTMR3	Myotubularin-related protein 3	Q8K296	Phosphatase	2 out of 4
PTPN8	Tyrosine-protein phosphatase non-receptor type 22	P29352	Phosphatase	3 out of 4
CDC14B	Dual specificity protein phosphatase CDC14B	Q6PFY9	Phosphatase	3 out of 4
Ppp2ca	Serine/threonine-protein phosphatase 2A catalytic subunit alpha isoform	P63330	Phosphatase	3 out of 4
PPEF2	Serine/threonine-protein phosphatase with EF-hands 2	O35385	Phosphatase	4 out of 4
PPP2R1A	Serine/threonine-protein phosphatase 2A 65 kDa regulatory subunit A alpha isc	Q76MZ3	Phosphatase	4 out of 4
ANP32E	Acidic leucine-rich nuclear phosphoprotein 32 family member E	P97822	Phosphatase Inhibitor	3 out of 4
PPP1R11	Protein phosphatase 1 regulatory subunit 11	Q8K1L5	Phosphatase Inhibitor	4 out of 4
PTK9	Twinfilin-1	Q91YR1	Transcription Regulation	2 out of 4
UBTF	Nucleolar transcription factor 1	P25976	Transcription Regulation	3 out of 4
RBAK	RB-associated KRAB zinc finger protein	Q8BQC8	Transcription Regulation	1 out of 4
NRF1	Nuclear respiratory factor 1	Q9WU00	Transcription Regulation	1 out of 4
LEF1	Lymphoid enhancer-binding factor 1	P27782	Transcription Regulation	1 out of 4
HOXB13	Homeobox protein Hox-B13	P70321	Transcription Regulation	1 out of 4
LDB2	LIM domain-binding protein 2	O55203	Transcription Regulation	1 out of 4
NFKB2	Nuclear factor NF-kappa-B p52 subunit	Q9WTK5	Transcription Regulation	1 out of 4
SUPT5H	Transcription elongation factor SPT5	O55201	Transcription Regulation	1 out of 4
GTF2F2	General transcription factor IIF subunit 2	Q8R0A0	Transcription Regulation	2 out of 4
SALL1	Sal-like protein 1	Q9ER74	Transcription Regulation	2 out of 4
FBXW7	F-box/WD repeat-containing protein 7	Q8VBV4	Transcription Regulation	2 out of 4
OVOL1	Putative transcription factor Ovo-like 1	Q9WTJ2	Transcription Regulation	2 out of 4
IRF3	Interferon regulatory factor 3	P70671	Transcription Regulation	2 out of 4
SMAD6	Mothers against decapentaplegic homolog 6	O35182	Transcription Regulation	3 out of 4
AATF	Protein AATF	Q9JKX4	Transcription Regulation	3 out of 4
UBTF	Nucleolar transcription factor 1	P25976	Transcription Regulation	3 out of 4
STAT3	Signal transducer and activator of transcription 3	P42227	Transcription Regulation	3 out of 4
E2F4	Transcription factor E2F4	Q8R0K9	Transcription Regulation	4 out of 4
GABPA	GA-binding protein alpha chain	Q00422	Transcription Regulation	4 out of 4
ELL	RNA polymerase II elongation factor ELL	O08856	Transcription Regulation	4 out of 4
BRCA1	Breast cancer type 1 susceptibility protein homolog	P48754	Transcription Regulation	4 out of 4
BRCA2	Breast cancer type 2 susceptibility protein homolog	P97929	Transcription Regulation	4 out of 4
FOXD3	Forkhead box protein D3	Q61060	Transcription Regulation	4 out of 4
GATA2	Endothelial transcription factor GATA-2	O09100	Transcription Regulation	3 out of 4
PHF12	PHD finger protein 12	Q5SPL2	Transcription Regulation	2 out of 4
SERTAD2	SERTA domain-containing protein 2	Q9JJG5	Transcription Regulation	1 out of 4
TAF10	Transcription initiation factor TFIID subunit 10	Q8K0H5	Transcription Regulation	4 out of 4
TAF6	Transcription initiation factor TFIID subunit 6	Q62311	Transcription Regulation	3 out of 4
TGIF	Homeobox protein TGIF1	P70284	Transcription Regulation	4 out of 4
Zfp236	Zfp236	B2RR24	Transcription Regulation	3 out of 4
ZFX	Zinc finger X-chromosomal protein	P17012	Transcription Regulation	3 out of 4
ETV5	ETS translocation variant 5	Q9CXC9	Transcription Regulation	1 out of 4
NUP62	Nuclear pore glycoprotein p62	Q63850	Transporter	1 out of 4
2610037M15RIK				3 out of 4
1190002A17RIK				3 out of 4
1110001A05RIK				4 out of 4
AA545217				4 out of 4
BC032967				2 out of 4
PLAGL2				2 out of 4
2810439M11RIK				3 out of 4
BC006779				3 out of 4
1500016H10RIK				4 out of 4
C130073D16RIK				2 out of 4
LOC216185				4 out of 4
SSBP4				1 out of 4

Supplemental table 1. siRNAs protecting against or sentizing to cisplatin in ES cells. List of siRNAs identified in primary screen (left column) and scoring in secondary confirmation screen (right column). Confirmed hits are indicated (3/4 confirmed, light blue; 4/4 confirmed, dark blue). Information in middle columns was acquired from Panther Classification System.

Supplemental table 2 (Not shown). Canonical pathways enriched in functional genomics, phosphoproteomics and transcriptomics datasets. List of molecules (right column) selected (IPA) in interaction-enriched networks derived from RNAi screen hits (light blue), differentially phosphorylated proteins (dark blue), or differentially expressed genes (green) that predict changes in canonical pathways (left column) falling into the categories cancer, cell cycle and survival, and differentiation.

Network	Molecules	Phosphopeptide	Phosphosite Position	Putative Motifs
p53 Signaling				
	ATM	_SPTFEEGSQGTTISSLSEK_	Ser1987	ATM/ATR
	BRCA1	_NINENPVSQNLK_	Ser1422	ATM/ATR
		TGSAQCMTQFVASENPK	Thr788	FHA KAPP
		TGSAQCMTQFVASENPK	Ser790	CAMK2
		ISNTPELTR	Thr1199	FHA2 Rad53p/Proline-directed
		SQGPVNPSPQR	Ser717	CDK1/CDK2/Proline-directed
	CHEK1	_FSSSQPEPR_	Ser317	ATM/ATR/CK2
	CTNNB1	_SPQMVSAIVR_	Ser196	ns
	EP300	_*AENVVEPGPPSAK_	Ser12	ns
	JMY	_SQAWAEGGSPR_	Ser108	CDK1/Proline-directed
	JUN	_NSDLLTSPDVGLLK_	Thr62	NEK6/Proline-directed
		NSDLLTSPDVGLLK	Ser63	CK2/FHA1 Rad53p
	MAPK14	_HTDDEMTGYVATR_	Thr180	ns
		HTDDEMTGYVATR	Tyr182	ns
		*SQERPTFYR	Ser2	ATM/ATR
	MDM2	_SLSFDPSLGLCELR_	Ser183	AURORA/AURORA-A/CAMK2/PKA/PKA/AKT
	MDM4	_TISAPVVRPK_	Ser368	CAMK2
		*TSHSTSAQCSASDSACR	Ser13	ns
	PIK3C2A	_SLSGATVTR_	Ser330	ns
	PML	_MESTEENEDRLATSSPEQSWPSTFK_	Ser503	CHK1
		MESTEENEDRLATSSPEQSWPSTFK	Ser504	CK2/PKD
	TOPBP1	_LQQADEDLLAQYGNDDSTMVEAK_	Ser498	CK2/PLK/PLK1
ATM Signaling				
	ATF2	_NDSVIVADQTPTPTR_	Thr51	Proline-directed
	ATM	_SPTFEEGSQGTTISSLSEK_	Ser1987	ATM/ATR
	BRCA1	_NINENPVSQNLK_	Ser1422	ATM/ATR
		TGSAQCMTQFVASENPK	Thr788	FHA KAPP
		TGSAQCMTQFVASENPK	Ser790	CAMK2
		ISNTPELTR	Thr1199	FHA2 Rad53p/Proline-directed
		SQGPVNPSPQR	Ser717	CDK1/CDK2/Proline-directed
	CHEK1	_FSSSQPEPR_	Ser317	ATM/ATR/CK2
	CREB1	_ILNDLSSDAPGVPR_	Ser143	ns
	JUN	_NSDLLTSPDVGLLK_	Thr62	NEK6/Proline-directed
	MAPK11	_QADEEMTGYVATR_	Tyr182	ns
	MAPK14	_HTDDEMTGYVATR_	Thr180	ns
		HTDDEMTGYVATR	Tyr182	ns
		*SQERPTFYR	Ser2	ATM/ATR
	MAPK9	_TACTNFMMTPYVVTR_	Tyr185	ns
	MDC1	_VLLAADSEEEGDFPS(ph)GR_	Ser176	ns
		DLEGLASAPIITGSQADGGKGDPLSPGR	Ser919	ATM/ATR/CK2
		SQSGSPAAPVEQVVIHTDTSGDPTLPQR	Ser592	ATM/ATR/GSK3
		VTDQSLTLQSSPLSASPVSSTPDLKPPVPIAQPVTPEPIPQANHQR	Ser1371	GSK3/NEK6/Proline-directed
	MDM2	_SLSFDPSLGLCELR_	Ser183	AURORA/AURORA-A/CAMK2/PKA/PKA/AKT
	MDM4	_TISAPVVRPK_	Ser368	CAMK2
	NBN	_GKTPSYQLSPMKFPVANK_	Ser433	CDK1/CDK2/CK1/Proline-directed
		NHAVLTVNFPVTSLSQTDEIPTLTIK	Ser58	ATM/ATR/CK2
		KLSQETFNIK	Ser398	ATM/ATR/CAMK2/CK1/PKA
	RAD50	_EAQLASSQEIVR_	Ser237	ATM/ATR/NEK6
		LFDVDGSQDLESDLGR	Ser635	ATM/ATR
	SMC2	_ASNLDDLVYK_	Ser60	PKA
	TLK1	_*SVQSSSGSLEGPPSWSR_	Ser9	CK1
		FTGVATGSTGSTGSCSVGAK	Ser80	CK1
	TLK2	_SSPQHSLSNPLPR_	Ser110	ns
		SSPQHSLSNPLPR	Ser117	ns
	TP53BP1	_LPADSENVLVTPSQDDQVEMSQNVDK_	Ser565	ATM/ATR/CK2
		SISAPVIFDR	Ser119	CK1
		LMLSTSEYSQSSK	Ser517	ATM/ATR/CK1
		APACASQSFCESSSETPFHFTLPK	Ser876	ATM/ATR
		SNISSPVTPTAASSSTTPTRK	Ser1623	CK1/ERK/MAPK/FHA KAPP/Proline-directed
		EQYGLGPYEAVTPLTK	Thr1594	Proline-directed
		QSEQPVKPVGPVMDDAAPEDSASPVSQQR	Ser1090	Proline-directed
		ASQEPFSPAEDVMETDLLEGLAANQDRPSK	Ser1103	CK2/ERK/MAPK/Proline-directed
RAR Activation				
	CSNK2A2	_VYAEVNSLR_	Ser18	ns
	EP300	_*AENVVEPGPPSAK_	Ser12	ns
	JUN	_NSDLLTSPDVGLLK_	Thr62	NEK6/Proline-directed
		NSDLLTSPDVGLLK	Ser63	CK2/FHA1 Rad53p
	MAP3K1	_AVQQPSSPQQPVAGSQR_	Ser518	ERK/MAPK/Polo box/Proline-directed
	MAPK11	_QADEEMTGYVATR_	Tyr182	ns
	MAPK14	_HTDDEMTGYVATR_	Thr180	ns
		HTDDEMTGYVATR	Tyr182	ns
		*SQERPTFYR	Ser2	ATM/ATR
	MAPK9	_TACTNFMMTPYVVTR_	Tyr185	ns
	NCOR1	_SPGSISYLPSFFTK_	Ser2199	CK1/Proline-directed
	NFKB1	_KLSFTESLTGDGSPLLSLNK_	Ser940	CAMK2/CK2/GSK3/PKA
	PDPK1	_SQTEPGSSPGIPSGVSR_	Ser38	Polo box/Proline-directed
	PML	_MESTEENEDRLATSSPEQSWPSTFK_	Ser503	CHK1
		MESTEENEDRLATSSPEQSWPSTFK	Ser504	CK2/PKD
	PRKACA	_TWTLCGTPEYLAPEIILSK_	Thr198	CAMK2
	PRKCI	_QVVPFKPNISGEFGLDNFDSQFTNEPVQLTPDDDDIVR_	Thr563	CK2/FHA1 Rad53p/Proline-directed
	SMARCA4	_KAENAEGQTPAIGPDGEPLDETSQMSDLPVK_	Ser610	ATM/ATR
		KAENAEGQTPAIGPDGEPLDETSQMSDLPVK	Ser613	CK1
	SNW1	_SLQTSLVSSR_	Ser33	CK1/GSK3/NEK6
	SRC	_LFGGFNSSDTVTSPQR_	Ser74	CDK1/CDK2/ERK/MAPK/Proline-directed
	TRIM24	_SILTSLLLNSSQSSASEETVLR_	Ser771	CK2/CK1
		SILTSLLLNSSQSSASEETVLR	Ser772	CK1
BMP-TGFβ Signaling				
	ATF2	_NDSVIVADQTPTPTR_	Thr51	Proline-directed
	CREB1	_ILNDLSSDAPGVPR_	Ser143	ns
	EP300	_*AENVVEPGPPSAK_	Ser12	ns
	JUN	_NSDLLTSPDVGLLK_	Thr62	NEK6/Proline-directed
		NSDLLTSPDVGLLK	Ser63	CK2/FHA1 Rad53p
	MAGED1	_AGPGTTYNFPQSPSANEMTNNQPK_	Ser213	ERK/MAPK/Proline-directed
	MAPK11	_QADEEMTGYVATR_	Tyr182	ns
	MAPK14	_HTDDEMTGYVATR_	Thr180	ns
		HTDDEMTGYVATR	Tyr182	ns
		*SQERPTFYR	Ser2	ATM/ATR
	MAPK9	_TACTNFMMTPYVVTR_	Tyr185	ns
Wnt Signaling				
	APC	_SGECSPVPMGSFPR_	Ser109	CK1/Proline-directed
	APPL1	_VNQSALEAVTPSPSFQQR_	Ser401	Proline-directed
	CSNK1A1	_*ASSSGSKAEFIVGGK_	Ser3	GSK3
	CSNK2A2	_VYAEVNSLR_	Ser18	ns
	CTNNB1	_SPQMVSAIVR_	Ser196	ns
	DVL2	_DLGSVPPELTASR_	Thr717	NEK6
	EP300	_*AENVVEPGPPSAK_	Ser12	ns
	GJA1	_SDPYHATTGPLSPSKDCGSPK_	Ser255	CDK1/CDK2/CK1/ERK/MAPK/Proline-directed
		SDPYHATTGPLSPSKDCGSPK	Ser257	NEK6
	JUN	_NSDLLTSPDVGLLK_	Thr62	NEK6/Proline-directed
		NSDLLTSPDVGLLK	Ser63	CK2/FHA1 Rad53p
	LRP6	_GTYFPALNPPPSPRATER_	Ser1490	ERK/MAPK/Proline-directed
	MARK2	_VPVASPSAHNISSSSGAPDR_	Ser566	ERK/MAPK/Proline-directed
	MDM2	_SLSFDPSLGLCELR_	Ser183	AURORA/AURORA-A/CAMK2/PKA/PKA/AKT
	PPP2R5D	_QSSFPFNLNK_	Ser82	CAMK2
	PPP2R5E	_*SSAPTTPPSVDKVDGFSR_	Thr7	ERK/MAPK/FHA KAPP/Proline-directed
	SRC	_LFGGFNSSDTVTSPQR_	Ser74	CDK1/CDK2/ERK/MAPK/Proline-directed
	TCF3	_AGAPSALSPNYDAGLHGLSK_	Ser378	CK1/Proline-directed

*Acetylation
ns: Not specified

Supplemental table 3. List of SILAC-derived differentially phosphorylated peptides in key CP-regulated signaling pathways. Phosphopeptides (differentially phosphorylated AA indicated in red), Phosphosite position number, and putative kinase motifs are shown. Differentially phosphorylated peptides are grouped in canonical pathways “p53 signaling”, “ATM signaling”, “RAR activation”, “Wnt/β-catenin signaling and BMP/ TGFβ signaling”.

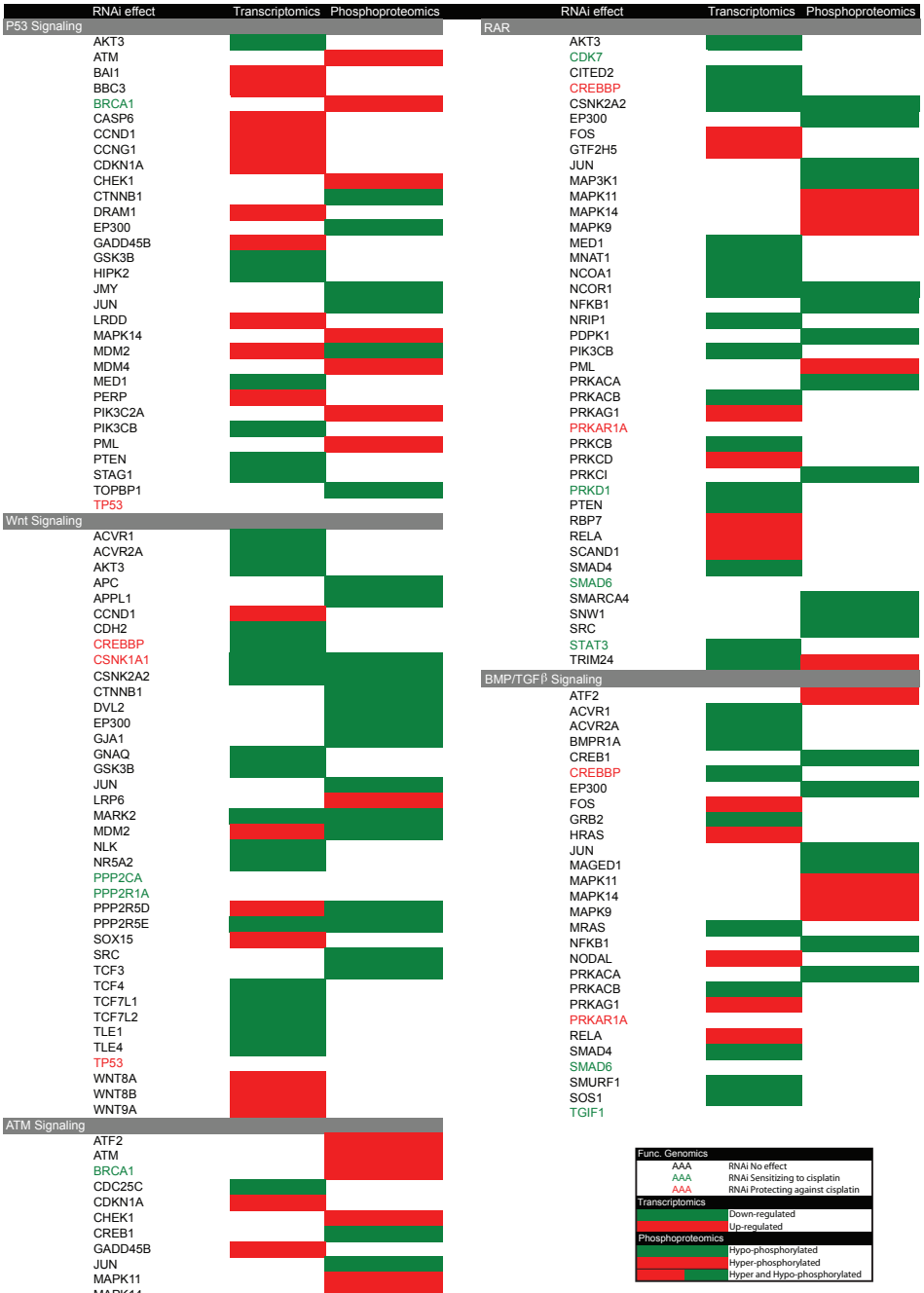

Supplemental table 4. Molecules identified by IPA in the signaling networks in common in the three OMICS data sets. Effect of siRNA (left column), behavior in micro-array (middle column) and behavior in SILAC (right column) shown for molecules identified by Ingenuity Pathway Analysis in the signaling networks depicted in Fig 5. Color-coding as indicated.